ORNL/SPR-2019/1128

Nuclear Data – Benchmarking $^{19}F(\alpha,n)$ Yield Data for Nuclear Safeguards

Stephen Croft
Ramkumar Venkataraman
Glenn Fugate
Ian Gauld
Robert McElroy
Angela Moore
Andrea Favalli
Daniela Henzlova
Martyn Swinhoe

September 2019

Approved for public release.
Distribution is unlimited.

OAK RIDGE NATIONAL LABORATORY
MANAGED BY UT-BATTELLE FOR THE US DEPARTMENT OF ENERGY

DOCUMENT AVAILABILITY

Reports produced after January 1, 1996, are generally available free via US Department of Energy (DOE) SciTech Connect.

Website www.osti.gov

Reports produced before January 1, 1996, may be purchased by members of the public from the following source:

National Technical Information Service
5285 Port Royal Road
Springfield, VA 22161
Telephone 703-605-6000 (1-800-553-6847)
TDD 703-487-4639
Fax 703-605-6900
E-mail info@ntis.gov
Website http://classic.ntis.gov/

Reports are available to DOE employees, DOE contractors, Energy Technology Data Exchange representatives, and International Nuclear Information System representatives from the following source:

Office of Scientific and Technical Information
PO Box 62
Oak Ridge, TN 37831
Telephone 865-576-8401
Fax 865-576-5728
E-mail reports@osti.gov
Website http://www.osti.gov/contact.html

This report was prepared as an account of work sponsored by an agency of the United States Government. Neither the United States Government nor any agency thereof, nor any of their employees, makes any warranty, express or implied, or assumes any legal liability or responsibility for the accuracy, completeness, or usefulness of any information, apparatus, product, or process disclosed, or represents that its use would not infringe privately owned rights. Reference herein to any specific commercial product, process, or service by trade name, trademark, manufacturer, or otherwise, does not necessarily constitute or imply its endorsement, recommendation, or favoring by the United States Government or any agency thereof. The views and opinions of authors expressed herein do not necessarily state or reflect those of the United States Government or any agency thereof.

ORNL/SPR-2019/1128

Nuclear Nonproliferation Division

NUCLEAR DATA – BENCHMARKING $^{19}F(\alpha,n)$ YIELD DATA FOR NUCLEAR SAFEGUARDS

Stephen Croft
Ramkumar Venkataraman
Glenn Fugate
Ian Gauld
Robert McElroy
Angela Moore*
Andrea Favalli**
Daniela Henzlova**
Martyn Swinhoe**

*University of Tennessee, Knoxville
**Los Alamos National Laboratory

September 2019

Prepared by
OAK RIDGE NATIONAL LABORATORY
Oak Ridge, TN 37831-6283
managed by
UT-BATTELLE, LLC
for the
US DEPARTMENT OF ENERGY
under contract DE-AC05-00OR22725

CONTENTS

LIST OF FIGURES

LIST OF TABLES

EXECUTIVE SUMMARY

The goal of this 1 year project was to measure the thick-target yield from the $^{19}F(\alpha,n)$ reaction in UF_6 with a high accuracy of approximately ±2%. This accuracy will be a significant improvement over currently available data in the literature which show a scatter of ±30%. The stated goal of establishing the specific yield (neutrons/sec/gram) of ^{234}U, a legitimate physical constant, was accomplished via direct measurements. Two recognized safeguards instruments were used to measure a diverse collection of well-characterized small samples—the Los Alamos National Laboratory (LANL) Mini-Epithermal Neutron Multiplicity Counter (Mini-ENMC) and the Oak Ridge National Laboratory (ORNL) Large-Volume Active Well Coincidence Counter (LV AWCC). The instruments are efficiency calibrated using a National Institutes of Standards and Technology (NIST)–certified ^{252}Cf source. A Monte Carlo transport code (MCNP)–based adjustment to the $F(\alpha,n)$ launch spectrum and items was made using spectra taken from the literature* as well as predicted by the SOURCES4C code. The SOURCES 4C codes makes use of thin target data, a nuclear model for energetics, and stopping power data. SOURCES 4C was updated for this case alone, namely, ^{234}U $^{19}F(\alpha,n)$ yields from UF_6 using the alpha stopping powers calculated using the SRIM code and a blended microscopic cross section data set. The blended microscopic cross sections consisted of data available to ORNL from a previous NA-22 project.† A robust determination of the n/s/g of ^{234}U in UF_6 was generated along with a scientifically defensible uncertainty analysis. The dominant sources of uncertainty are efficiency determination (1.1% relative standard deviation associated with the ^{252}Cf reference source) and an additional about 0.9% systematic uncertainty coming from the uncertainty in the $F(\alpha,n)$ spectrum. The combined overall relative uncertainty is of the order of 2%.The stated uncertainties are an order of magnitude better than current data based on accelerator data reported in the literature. The updated SOURCES 4C code is available to the safeguards community and beyond from the Radiation Safety Information Computational Center (RSICC) at ORNL, which is a repository for computer codes used in the field of nuclear technology. The ^{234}U $^{19}F(\alpha,n)$ yield from UF_6 established in this project will be shared with the NDA Working Groups associated with the Institute of Nuclear Material Management (INMM) and the European Safeguards Research and Development Association (ESARDA). The updated yield and the publications related to this work will be included in the next revision of the relevant ASTM C26.10 and ANSI N15 standards. Aside from being of immediate and direct use by the safeguards community, the ^{234}U $^{19}F(\alpha,n)$ yield from UF_6 established in this project will serve as an enduring integral benchmark that subsequent data evaluations will need to match in order to be credible.

---

* GJH Jacobs and H Liskien, "Energy Spectra of Neutrons Produced by α-Particles in Thick Targets of Light Elements," *Annals of Nuclear Energy* 10(10) (1983) 541-552.

† W.A. Peters et al., *A kinematically complete interdisciplinary and co-institutional measurement of the $^{19}F(\alpha,n)$ cross section for nuclear safeguards science*, Idaho National Laboratory Report INL/EXT-16-38791.

ABSTRACT

Fluorine compounds of U and Pu are ubiquitous in the nuclear fuel cycle, so F(α,n) neutrons are an important signature and quantitative source term that needs to be understood for physics-based interpretation of nondestructive assay measurements. Historically there have been large differences in the basic nuclear data for this reaction reported by various groups. UF_6 is the most prominent material in the nuclear fuel cycle, with the potential for short-term production into weaponizable form. Verification of bulk quantities, natural feed, depleted tails, and especially low enriched product in cylinders is particularly important. The principal physical measurement is neutron counting. For enriched material, the $^{19}F(\alpha,n)$ reaction, driven by ^{234}U, is the dominant source of neutrons. Basic nuclear data, cross sections, needed to calculate the yield, as well as information on the source spectrum for sensitivity studies are sparse and highly discrepant. This limits defensible physics-based performance evaluations. The same applies to holdup and criticality studies in which hydrated uranyl fluoride is the material of interest which accumulates in enrichment facilities. In the future we anticipate that the physics community will have made improved accelerator-based measurements and undertaken a more thorough evaluation and adjustment of all relevant available data. But in the short term, this does not help the safeguards community face the pressing real-world nondestructive assay requirements. To address this need, we have performed quality neutron measurements on UF_6 materials using well-known material and high-capability neutron counters. A robust determination of the n/s/g of ^{234}U in UF_6 was generated along with a scientifically defensible uncertainty analysis. The weighted average value of the neutron yield is 509 n/s/g^{234}U with a random uncertainty of approximately 1%. Dominant sources of systematic uncertainty are in the efficiency determination where we incur approximately 1.1% relative standard deviation associated with the ^{252}Cf reference source and about 0.9% uncertainty coming from the uncertainty in the F(α,n) spectrum. The stated uncertainties are an order of magnitude better than current data based on accelerator data reported in the literature. Aside from being of immediate and direct use by the safeguards community, this result will serve as an enduring integral benchmark for subsequent data evaluations that will need to match it in order to be credible. In addition to yield normalization, safeguards users of F(α,n) data also need guidance of the neutron emission spectrum. We have generated a neutron emission using a modified version of the well-known SOURCES 4C code, updated with new alpha stopping power coefficients, and a blended microscopic cross section data set. The yield and spectra are available in a form that MCNP users can readily use.

1. INTRODUCTION

Thick-target integrated over angle (α,n) yields and neutron emission spectra for special nuclear materials in a variety of compounds are needed to help interpret nuclear safeguards measurements. For instance, when ^{nat}U is enriched using a method that exploits the mass difference between UF_6 molecules, ^{234}U is also enriched in the product stream [1-4]. Consequently, the low enriched uranium (LEU) hexafluoride, collected and stored in product cylinders prior to its processing into reactor fuel, is a relatively strong source of F(α,n) driven predominately by ^{234}U. Measurement of the neutron rate emerging from storage cylinders is routinely used to verify their declared content. Even assuming commercial enrichment facilities are optimized to closely approximate an ideal cascade, the ^{234}U mass fraction enrichment as a function of ^{235}U mass fraction enrichment will still vary depending on the enrichment of the tails (which is driven by economics) and the ^{234}U content of uranium ores (which can vary over an approximate range of 48 to 62 ppm) [1]. The natural variability in the $^{234}U/^{238}U$ atom ratio is attributed to ^{234}U and ^{238}U not being in secular equilibrium [5] due to water leaching at radiation-damaged lattice sites. Neutron measurements therefore also rely on isotopic composition data, either measured or based on a correlation with enrichment.

Such measurements are an important part of the overall system of nuclear safeguards measures that are in place to verify that enrichment facilities, and the materials they process are being used only for peaceful purposes. This is important because in terms of separative work, LEU uranium hexafluoride is an attractive feed material for the production of highly enriched uranium (HEU).

In contrast to the passive gamma signatures, which come mainly from the outermost surface or *skin*, the emergent neutron intensity is more representative of the bulk content of the cylinder. Because of this, and because passive neutron counting is simple and stable, neutron counting has long been recognized to be an attractive nondestructive way to assay the amount of ^{235}U present [6]. Although it is most common to use direct neutron measurements [7], indirect neutron signatures such as the detection of capture gamma-rays generated in steel are also viable [8]. Both techniques are candidate technologies for inclusion in unattended cylinder verification stations at centrifuge enrichment plants [9].

We note that for similar reasons neutron counting is the preferred method for the measurement of uranium holdup inventory in large components of gaseous diffusion cascades. In this case, uranyl fluoride (UO_2F_2:nH_2O), the reaction product of UF_6 with moist air, is usually considered the compound of interest, with F(α,n) being the principal source term. For the Oak Ridge Gaseous Diffusion Plant, the cascade allowed for various arrangements, with feed and product withdrawal to occur at different locations and

with cell and unit bypass. As a result, ^{234}U correlations based on sampling by building were developed [2], although the question of what value to use for the n/s/g ^{234}U remained [10] given the long-standing inconsistencies in the knowledge of the F(α,n) cross section and yield curve in various compounds [11].

The purpose of our measurements is to support a science-based approach by measuring the specific (α,n) yield, in neutrons per second per gram of ^{234}U in UF_6. To do this, we use two recognized safeguards instruments: the Los Alamos National Laboratory (LANL) Mini-Epithermal Neutron Multiplicity Counter (mini-ENMC) and the Oak Ridge National Laboratory (ORNL) Large-Volume Active Well Coincidence Counter (LV AWCC) to measure a diverse collection of well-characterized small samples. The instruments are efficiency calibrated using a National Institutes of Standards and Technology (NIST) certified ^{252}Cf source. An MCNP adjustment to the F(α,n) launch spectrum and items is made using spectra taken from the literature as well as predicted by the SOURCES4C code [12]. Our initial goal was to make a determination with a defensible uncertainty (1-σ) of less than about 2%. This is over an order of magnitude better than the scatter in literature values (see review [11]). Three measurement campaigns have been conducted. Here we will report results using only the LV AWCC from the first two campaigns and for the items measured individually, as the other data are still being analyzed.

The present measurement also serves as a high-quality benchmark for future data evaluation which combines thin target (differential), thick target, and integral information about the F(α,n) reaction.

2. ACHIEVEMENT OF PROJECT GOALS ON A TASK BY TASK BASIS

This section describes the work performed on the various tasks and the goals accomplished.

2.1 TASK 1: MEASUREMENT OF WELL-KNOWN UF_6 ITEMS USING STANDARD NEUTRON COUNTERS

The purpose of our measurements was to support a science-based approach by measuring the specific (α,n) yield, in neutrons per second per gram of ^{234}U in UF_6. To do this, two recognized safeguards instruments were used to measure a diverse collection of well-characterized small samples: LANL Mini-mini-ENMC and the ORNL LV AWCC. Several UF_6 items of well-known enrichments and mass loadings were measured. The ORNL LV AWCC is similar in design to the standard AWCC (Canberra Industries Inc., model JCC-51 [13]) but has been scaled to a larger cavity diameter and uses higher pressure neutron detectors. It uses 48 ^{3}He-filled cylindrical proportional counters [GE RS-P4-08P4-202] of 25.4 mm (1 inch) external diameter, 0.508 mm stainless steel wall thickness with a ^{3}He partial pressure of 4.5 atm at 25°C and 635 mm (25 inches) active length arranged in two concentric rings about an 11 inch diameter, 15 inch tall assay measurement cavity. For the measurements in this task, graphite end-

plugs were used with an internal 0.5 mm thick Cd layer. A photograph of the LV AWCC is shown in Figure 1.

Figure 1. The ORNL LV AWCC.

The mini-ENMC has a split sample cavity that enables the counter to be configured as a well counter or opened to accommodate samples larger than the measurement cavity. The outer dimensions of the mini-ENMC are 56 cm by 56 cm by 89 cm high. The closed geometry sample cavity is 15.9 cm in diameter by 38 cm high. There are 104 ^{3}He tubes filled to 10 atmosphere pressure (52 in each half) arranged in four concentric rings. The inner cavity is lined with cadmium, and cadmium also surrounds the outermost ring. Figure 2 shows an MCNP drawing of the tube arrangement and the counter and a picture of the counter in the open configuration.

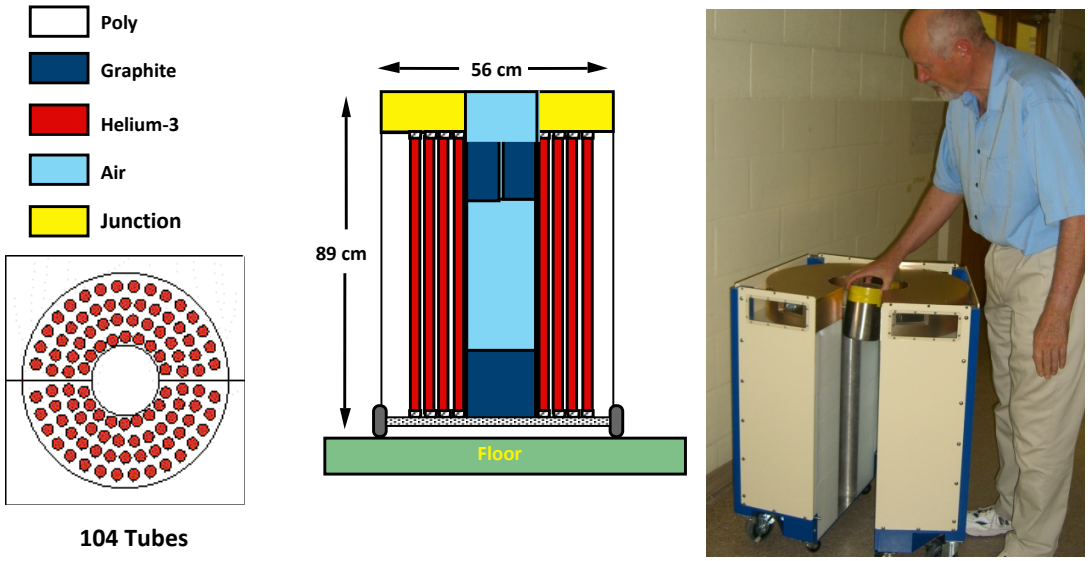

Figure 2. Schematic drawings and picture of LANL mini-ENMC.

Various chemically pure UF_6 items were counted several times, individually and in combination (some were included in all three campaigns as an internal consistency check). This was done to include as much non-controlled variation as possible into the data set so that the overall uncertainty is realistic. The samples measured were three P-10 cylinders, each containing about 15 g of 90% enriched UF_6; three 1-S cylinders, each containing about 400 g of UF_6 at 4.6% enrichment; and two 2-S cylinders of about 400 g UF_6 each, with enrichments of 2.7 and 4.6 % respectively; pseudo-hoke stainless steel items, New Brunswick Laboratory (NBL) cylinders with LEU; and a depleted uranium (DU) keg. The items shown in Figure 3 (from left to right) are, 1S cylinder, the NBL-22 cylinder, the NBL-7 cylinder, a pseudo-hoke stainless steel item, two P-10 cylinders, and the DU keg. The purity, enrichment, and UF_6 mass of each item were accurately known by analytical chemistry methods. The items differed substantially in ^{234}U enrichment (for example three pseudo-hoke stainless steel items with 0.87, 1.4, and 2.2 at% ^{234}U). Multiple measurements were taken in two campaigns separated by a number of months, so that the background and other effects were realistically sampled. The spontaneous fission and cosmic ray spallation contributions for all samples were negligible. Further, the neutron signal was dominated by ^{234}U-induced (α,n) reactions. The allowance for ^{235}U plus ^{238}U (α,n) contributions was only 2.8, 1.4, and 0.81 % in ascending order of ^{234}U abundance. Collectively the items provided a check on the robustness of the analysis.

Figure 3. Various items available for measurement. In the photograph the P-10 configurations are shown in the second column from the right, and an example of the Hoke container is the third column from the right.

The mass loadings are given in Table 1.

Table 1. Mass loadings and enrichment of UF_6 items.

Item(s)	Gross	Tare	Net	unc.	Container material	Enrichment ^{235}U
	g	g	g	g		
NBL22			406.83	0.01	Monel	4.6138
NBL7			1875.4	0.01	Monel	2.7326
DU			670.9	0.1	Maraging Steel	0.2914
P-10			3.645		KEL-F	90.073
ANL-10	373.4	358.6	14.79	0.005	STST	90.073
ANL-11	346.9	332.1	14.79	0.005	STST	90.123
ANL-12	369.2	354.4	14.79	0.005	STST	90.152
Sum	1089.5	1045.1	44.37			
1S-1	1729	1312.3	416.69		Ni or Monel	4.6148
1S-2	1761.1	1360.8	400.31		Ni or Monel	4.6148
1S-3	1758.7	1314.4	444.25		Ni or Monel	4.6148

Besides counting UF_6 items by themselves, a NIST traceable ^{252}Cf source was counted for the purposes of determining the measured efficiency of the counter for the ^{252}Cf energy spectrum.

2.2 TASK 2: BENCHMARKING MCNP EFFICIENCIES USING A NIST-CERTIFIED ^{252}CF SOURCE

Recently it has been realized that absolute neutron coincidence counting (NCC) has the potential to determine the neutron production rate in ^{252}Cf sources to high accuracy. The ABsolute Californium Determination (ABCD) method using NCC allows users to independently check the emission rate of a certified source (which is always a good experimental practice), or, in some circumstances, perhaps even self-certify a source at a similar or higher level of accuracy as a national metrology laboratory. The primary reference source used in this work was FTC-CF-1830, and we adopted the emission rate established by the U.S. National Institute of Standards and Technology (NIST) using their $MnSO_4$ bath. But as a check we undertook the absolute NCC measurement described in Appendix A. This is an important aspect of the present $UF_6(\alpha,n)$ measurement campaign because it independently confirms the absolute scale of the measurements.

The limited objective of the present Cf-yield determination measurements was to provide an independent check on the certificate provided by NIST for FTC-CF-1830, since this source was used to set the absolute scale of our $UF_6(\alpha,n)$ specific yield determination. We consider checking the purity and yield of reference sources to be a good experimental practice in order to avoid unidentified error. Within the combined overall uncertainties stated, our assessment agrees with the decay-corrected calculation, so we have full confidence in the certificate value, which we have therefore adopted in the analysis of our $UF_6(\alpha,n)$ data. Several suggestions for improvements to the method of source strength measurement by the ABCD method using NCC described here can be offered because, according to the uncertainty analysis presented, the method is potentially capable of high accuracy, and our goal was not to approach the ultimate accuracy limit. To do so it is necessary to pay particular attention to all experimental steps and analysis details. The benefit of highly developing the ABCD technique for ^{252}Cf sources would be the resulting fillip it would provide to the entire applied neutron metrology community. Standardized high-density polyethylene moderated arrays for use by standards laboratories would be complementary to the established $MnSO_4$-bath technique but are in many ways easier to set up, maintain, and operate. Furthermore, it would be especially suitable for the weaker sources which challenge the detection limit of the $MnSO_4$ bath. NCC's are extremely stable and well suited to also make relative comparisons of all types of sources (not just ^{252}Cf). We also extend the analysis to show how the detection efficiency can also be estimated absolutely and directly using a small, sealed radionuclide ^{252}Cf source.

The measured efficiency from the NIST-certified ^{252}Cf source is used to determine the efficiency of the neutron counter for $^{19}F(\alpha,n)$ neutrons.

$$\varepsilon_{F(\alpha,n)} = \left(\frac{\varepsilon_{F(\alpha,n)}}{\varepsilon_{Cf252}}\right)_{MCNP} * \varepsilon_{Cf252\_measured} \cdot \quad (1)$$

2.3 TASK 3: MCNP SIMULATION OF LV-AWCCC AND MINI-ENMC TO SELECT A SUITABLE NEUTRON SPECTRUM BY MATCHING THE RING RATIO DATA

The efficiency calculations were performed using the Monte Carlo code MCNP. The MCNP model for the counters was updated to include UF_6 source geometries of interest. The model captured the details of the source(s) as well as any support structures such as a lab-jack that may have been used to locate the item inside the counter well. In the MCNP model, as well as in the measurements, the ^{252}Cf source was attached to the given UF_6 item at various locations (top, middle, bottom) and the variation in the efficiency was estimated. In all cases, the variation in the efficiency was negligible and well within the counting precision of a few tenths of a percent. Figure 4 and Figure 5 show the MCNP models of the LV-AWCC and the mini-ENMC, with the 1S-monel UF_6 item and the ^{252}Cf source attached toward the top of the item.

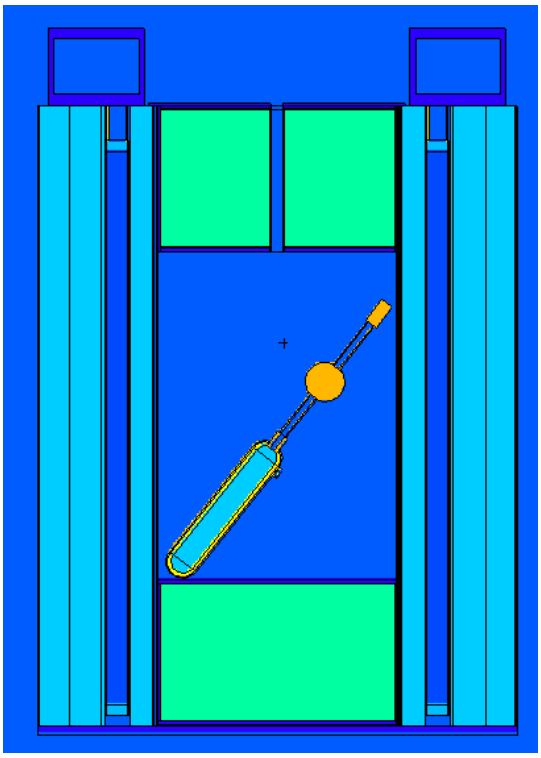

Figure 4. LV-AWCC with 1S-Monel UF_6 cylinder.

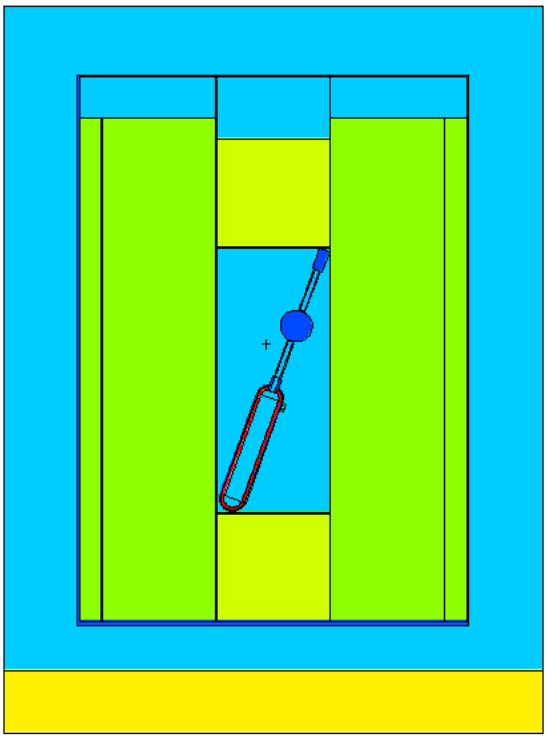

Figure 5. Mini-ENMC with 1S-Model UF_6 cylinder.

The efficiency was measured for each configuration using a NIST-certified ^{252}Cf spontaneous fission source (S/N FTC-CF-1810). The spectrum for ^{252}Cf neutrons was taken from the 71-energy-group Mannhart evaluation [14]. The absolute emission rate of the source has a relative 1-σ uncertainty of about

1%. Counting precision was negligible. Variation across the spatial extent of the items was typically less than 1% and represented a random uncertainty item to item because the exact distribution of UF_6 inside the cylinders is not known exactly. The items were stored on their sides, so thermal migration of the material inside might be expected to result in material along the length. The P-10 containers are transparent, and the UF_6 can be clearly seen to be concentrated into a small plug at the top. The efficiency for emerging F(α,n) neutrons was estimated by multiplying the measured efficiency value for ^{252}Cf by the calculated ratio of the efficiency of F(α,n) neutrons to ^{252}Cf neutrons. Because there was no evaluated F(α,n) spectrum, we adopted experimental results measured by Jacob and Liskien [15] for CaF_2 targets, measured by neutron Time-of-Flight at the laboratory in Geel, Belgium, in 0.1 MeV wide bins. The value of the MCNP calculated efficiency ratio was between 1.11 and 1.13 depending on the item. The uncertainty in the ratio due to spectral uncertainty was estimated to be about 0.63%. This was based on a sensitivity study in the case of the Jacob and Liskien data and a propagation of the full covariance in the case of the Mannhart spectrum. The uncertainty in the ratio is dominated by the treatment of the F(α,n) spectrum. The Jacob and Liskien data are available in histogram form with a bin width of 0.1 MeV. However, below 0.3 MeV their experimental method has limited analytical power, so a simple flat extrapolation was assumed in all cases. The model error (MCNP representation error) is expected to be small since this is a relative calculation. By using a low- and a high-fidelity model, we confirmed that the dependence on the geometrical representation was less than 0.6 %.

As an example, results for the ^{252}Cf efficiencies are shown in Figure 6 and Figure 7 for the UF_6 item P-10, for the LV-AWCC and the mini-ENMC.

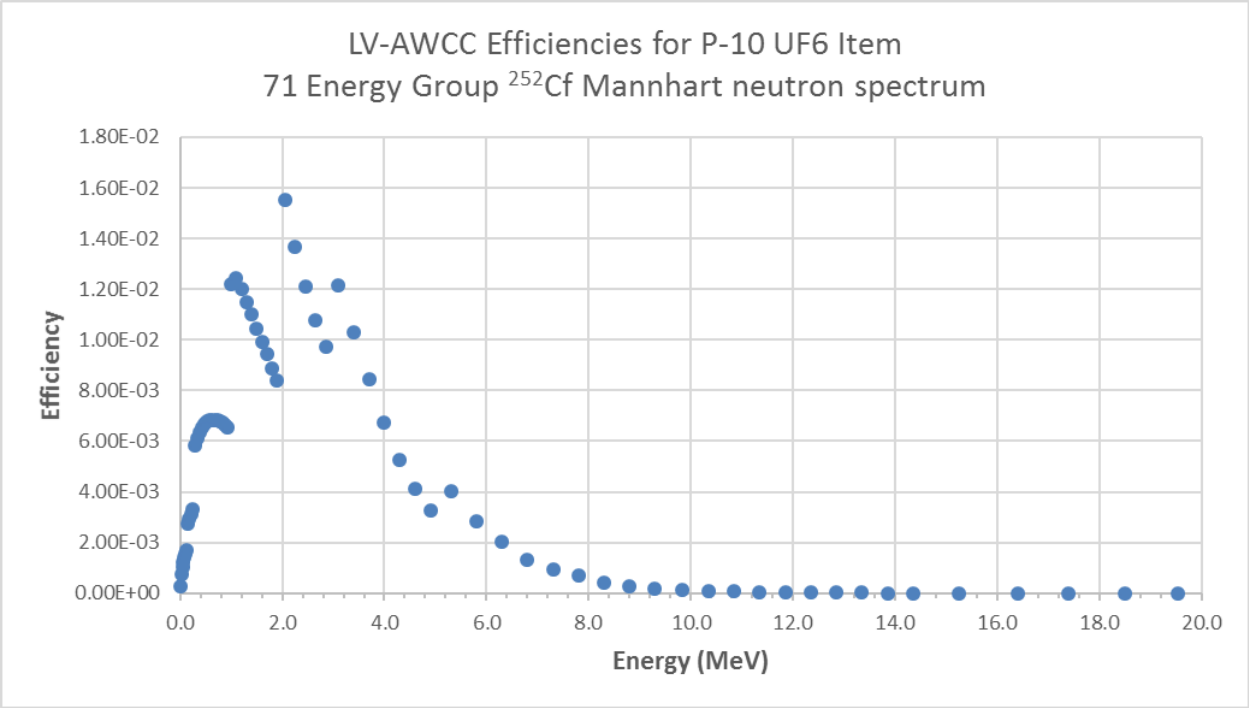

Figure 6. MCNP Efficiencies for LV-AWCC for UF_6 item P-10 – ^{252}Cf Mannhart Energy Spectrum.

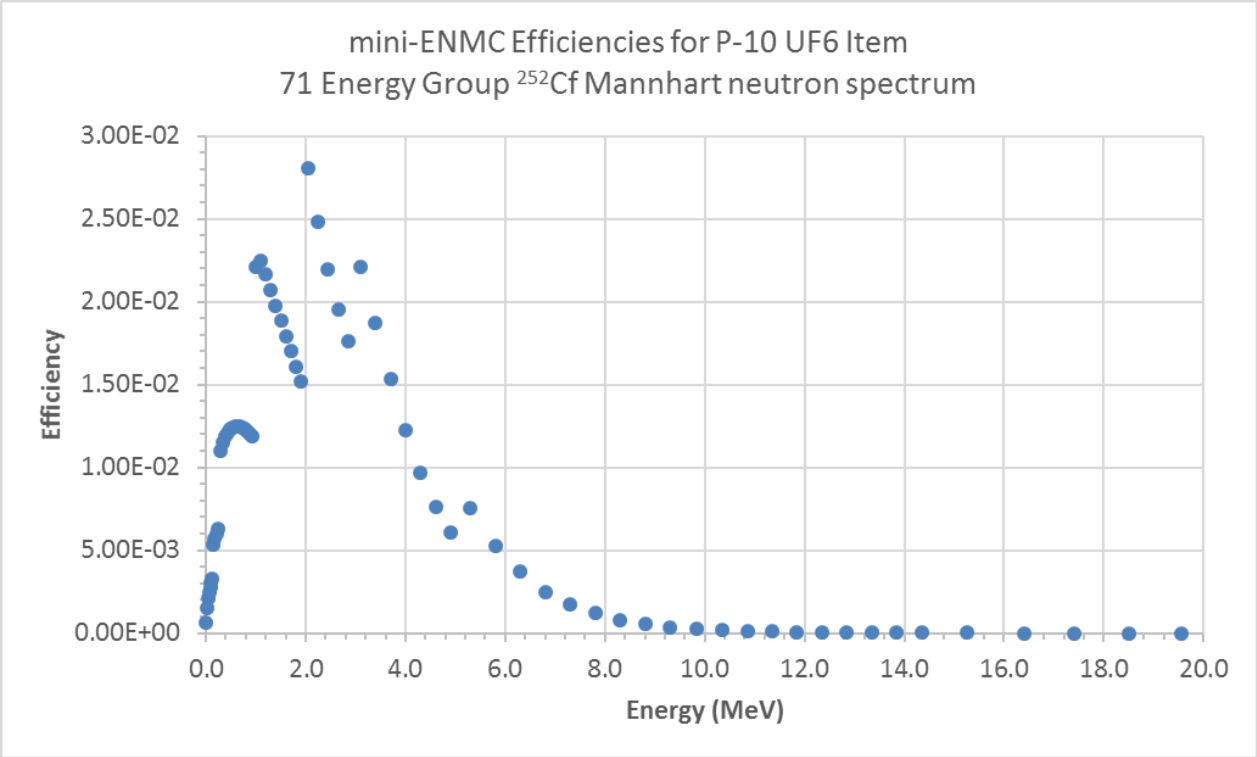

Figure 7. MCNP Efficiencies for mini-ENMC for UF6 item P-10 – ^{252}Cf Mannhart Energy Spectrum.

The plots show the fractional number of events registered in the detector at each energy bin, not the probability per unit energy. This is the reason for the apparent structure observed in Figure 6 and Figure 7. For the P-10 item, the LV-AWCC MCNP efficiency averaged over the normalized ^{252}Cf Mannhart energy spectrum ($\sum_{i=1}^{71}\varepsilon_i$) is 0.3438 ± 0.0001 counts/neutron; ε_i is the efficiency of the counter for the fraction of neutrons in the i-th energy bin. The mini-ENMC MCNP efficiency for the same item is 0.6289 ± 0.0001 counts/neutron. Uncertainties are sampling only at 1σ.

2.4 TASK 4: PROVIDE LAUNCH SPECTRUM OPTIONS FOR MODELING. IN ADDITION TO GUIDING THE CHOICE OF EFFICIENCY, THIS WILL BOUND THE EFFICIENCY UNCERTAINTY

It was noted earlier that because there is no evaluated F(α,n) spectrum, we adopted experimental results measured by Jacob and Liskien [15] for CaF_2 targets, measured by neutron time-of-flight at the laboratory in Geel, Belgium, in bins 0.1 MeV wide. By SOURCES4C calculation we showed that the difference between CaF_2 and UF_6 targets is not important from the point of view of the emitted spectrum. Jacob and Liskien provide data at 4, 4.5, 5 and 5.5 MeV incident alpha energy. We took the average of the 4.5 and 5 MeV spectra to be representative of that which would result from the ^{234}U line spectrum (average about 4.76 MeV). We took the 4.5 MeV spectrum to be "soft" (mean energy 1.0 MeV) and the 5 MeV spectrum to be "hard" (mean energy 1.12 MeV) and half the spread in calculated efficiency values to be indicative of the uncertainty associated with the uncertainty. MCNP sampling statistics were small (0.04% rsd) compared to the spectral uncertainty (0.67 to 0.77 % relative), which is the dominant uncertainty in the relative efficiency estimate.

We adopt experimentally based spectra for the UF_6 (α,n) spectrum, rather than the theoretically calculated spectra of SOURCES4C, because calculating the spectrum requires (among other nuclear data but in particular) detailed knowledge of the partial differential cross section, which is lacking [17]. The situation is rather complicated, as has been summarized by Bell et al. [18], and their results and insightful comments serve as a reminder not to accept model assumptions without some experimental verification and validation. The threshold for the ^{19}F(α,n)^{22}Na$^{g.s}$ reaction is approximately 2363 keV, but even though the ^{234}U α-line spectrum is relatively soft (4774 keV with probability 0.714; 4722 keV with probability 0.284, and 4602 with probability 0.02), the first seven states of ^{22}Na are energetically accessible. The situation is summarized in Table 2.

Table 2. States accessible in ^{22}Na by the ^{19}F(α,n) reaction stimulated by ^{234}U α-particles.

[Based on the List of Levels from www.nndc.bnl.gov]

Level, n	Level Energy (keV)	Alpha Particle Threshold Energy (keV)	Maximum Neutron Energy (keV)
0	0	2363.5	2467.4
1	583.1	3069.5	1826.1
2	657.0	3159.0	1743.6
3	890.9	3442.2	1480.3
4	1528.1	4213.8	733.4
5	1936.9	4708.8	175.4
6	1951.8	4726.9	148.3
7	1983.5	4765.3	76.6

The efficiency variation between items was not strong—0.3876, 0.3832, and 0.3874 counts/n for the P-10, ANL-11, and 1-S items, respectively. The uncertainty in the absolute efficiency scale is by the uncertainty in the ^{252}Cf calibration certificate (1.1%). The precision on the different sample rate determination is subject to a statistical replication uncertainty estimated from the scatter between measurements done at different times. It is on the order of 1% for the items measured individually.

2.4.1 Construction of a Thick-Target Yield for UF_6

From an intricate analysis of an ambitious and novel physics experiment, Peters et al. [19] have recently reported a new cross section measurement covering the range 3.92 to 6.67 MeV with reasonably fine energy resolution. If we consider this with other thin target data available in the scientific literature, we can construct the yield curve, $Y(E)$, for the two-component compound UF_6 by calculation according to

$$Y(E) = \left(\frac{n_1}{n_1 + n_2}\right) \cdot \int_0^E \frac{\sigma(E)}{\bar{\varepsilon}} \cdot dE, \tag{2}$$

where $n_1 = 6$, the number of F-target atoms per molecule, and $n_2 = 1$, the number of U atoms which do not undergo (α,n) reactions. $\sigma(E)$ is the microscopic ^{19}F(α,n) cross section, and $\bar{\varepsilon}$ is the stopping cross section per atom of the UF_6 molecule, which may be conveniently calculated using the SRIM-2013 [20] utility.

To construct the (α,n) cross section from threshold we have made the arbitrary choice to accept the values of Peters et al. from 3.92 to 6.67 MeV as reported; that is, they set the absolute scale. At and below 3.9122 MeV and including to 3.1043 MeV, we use the data of Balakrishnan et al. [21] scaled by 1.34. From threshold up to and including 3.10054 MeV, the data of Wrean and Kavanagh [22] scaled by a

factor of 2.68 is adopted. In this way the cross section is defined by 579 points from a threshold at 2.3635 MeV to 6.67 MeV. Above 6.67 MeV we extend the cross section to 9.92 MeV using 13 additional points extracted from the thick-target measurements of Norman et al. [23, 24] scaled by a factor of 1.14. We recognize that this approach is largely subjective and unsatisfactory since the individual data sets appear to be fundamentally incompatible in both scale and shape (beyond resolution differences). And we note the very large (non-unity) scaling factors needed to join the different data sets smoothly, that is, to stich them together on the scale defined by Peters et al. [19]. The result is shown is Figure 8. Note that this is the total cross section but tells nothing about the differential partial cross sections, which are needed to make spectral calculations (based on two-body reaction kinematics). At the present time it is common practice to turn to theoretical statistical model calculations for *guidance* on how to roughly partition the total cross section. This discussion emphasizes that a considerable amount of work remains to be done.

Performing the yield-curve integration using simple panel integration on the energy grid of the cross section data results in the yield curves, as shown in Figure 9. For the present discussion we have deliberately limited the plot to show only the energy range relevant to $^{234,\,235,\,238}$U α-particles. Plutonium materials and other measurement problems extend this range of interest. Also shown in the plot is the yield curve adopted in prior work [25] updated to SRIM-2013 stopping cross sections. The current curve shows a finer structure. Spectral changes might also be anticipated.

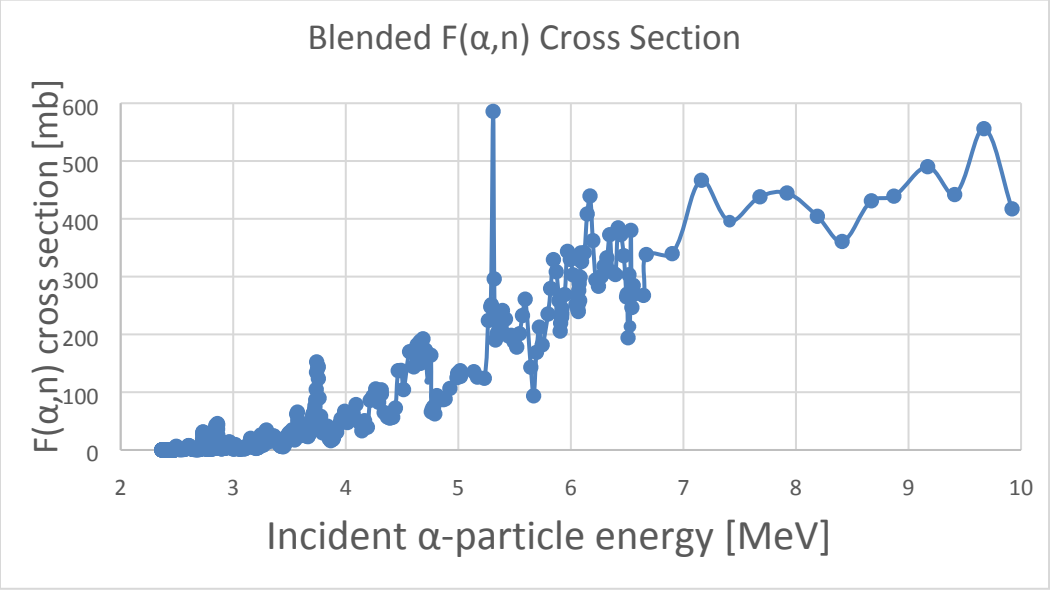

Figure 8. Blended microscopic ^{19}F(α,n) cross section σ(E) in mb as a function of incident α-particle energy in the laboratory frame, E, in MeV.

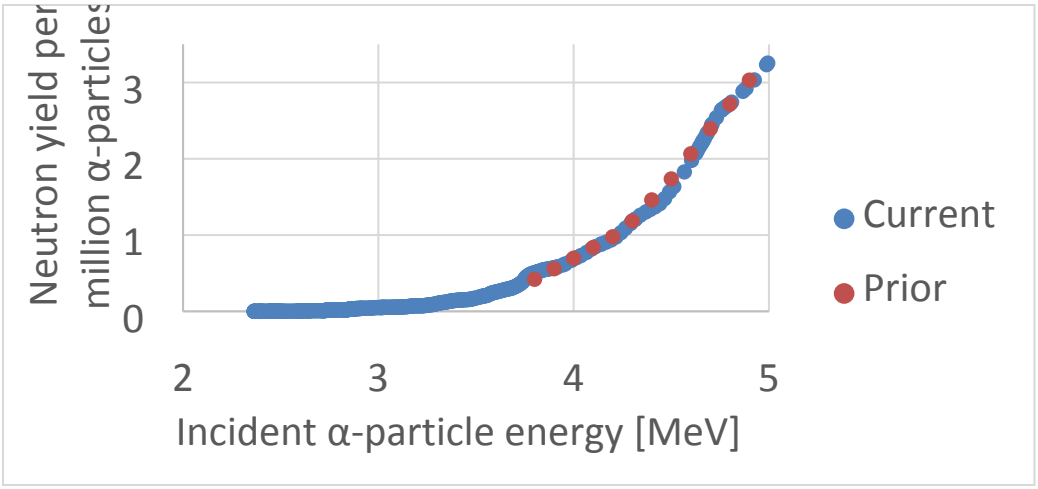

Figure 9. Calculated thick-target integrated over angle yield curve Y(E) in units of neutrons per million α-particles as a function of energy E, in MeV. The curve labelled "Current" is the result of the present work. The curve labelled "Prior" is based on an earlier estimate [25] that relies on the yield data of PbF_2 by Norman et al. [23–24] reanalyzed using SRIM-2013 stopping cross sections.

We highlight the impact of different stopping power tables and prescriptions. SOURCES 4C uses stopping powers from Ziegler (1977) [20]. In our work we have adopted SRIM-2013.These different data sources are by the same group. Figure 10 shows the ratio of the alpha stopping power for UF_6 computed using SRIM-2013 divided by the same quantity calculated using the Ziegler'77 algorithm. In the energy range of interest (above the threshold at 2.36 MeV and up to the alpha launch energies from U), the deviation from unity is on the order of 3%. This means that by using the same F(α,n) microscopic cross section data the computed thick-target yields would be about 3% lower when using SRIM-2013 stopping powers. Our present experimental accuracy for the ^{234}U in UF_6 yield is sub 2%, so it is clear updates to the SOURCES 4C code are needed. This also emphasizes the need to measure the yield from different compounds directly and to measure stopping powers in compounds of interest directly, because undoubtedly there will be a bias in SRIM-2013 in addition to binding and additivity assumption errors.

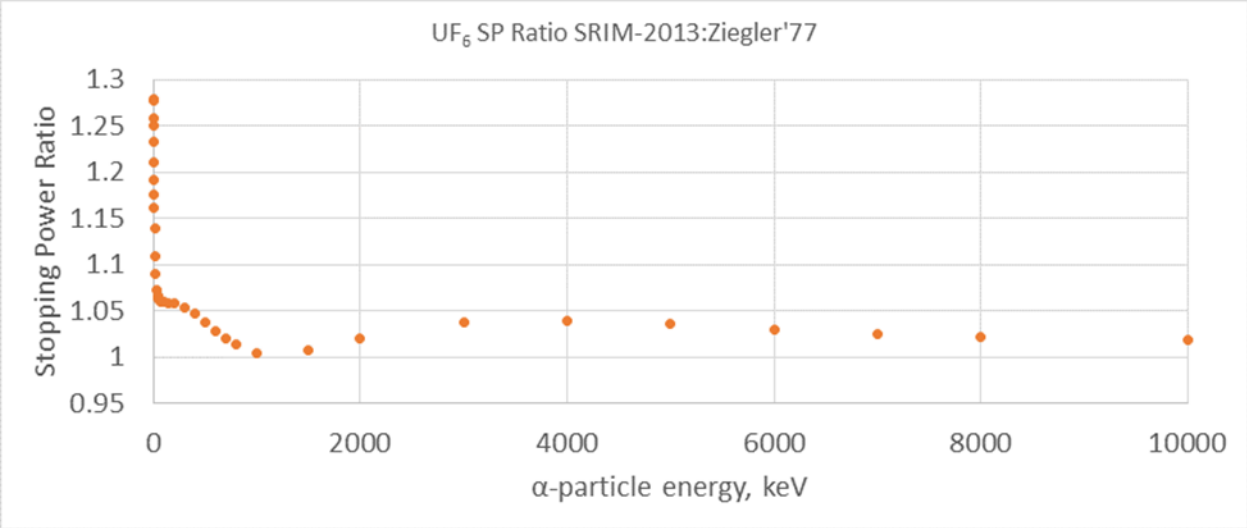

Figure 10. Ratio of alpha stopping powers of UF_6; SRIM-2013 to Ziegler-1977.

2.4.2 Discussion on Neutron Spectra Calculated Using SOURCES 4C; Updated MCNP efficiencies

The SOURCES 4C code was updated (for UF_6 only) using the blended microscopic F(α,n) cross section data set and the alpha stopping coefficients. Using these, (α,n) launch spectra were calculated for ^{234}U, ^{235}U, and ^{238}U in energy bins 0.1 MeV wide. Figure 11 shows the F(α,n) launch spectra calculated using the updated SOURCES 4C code.

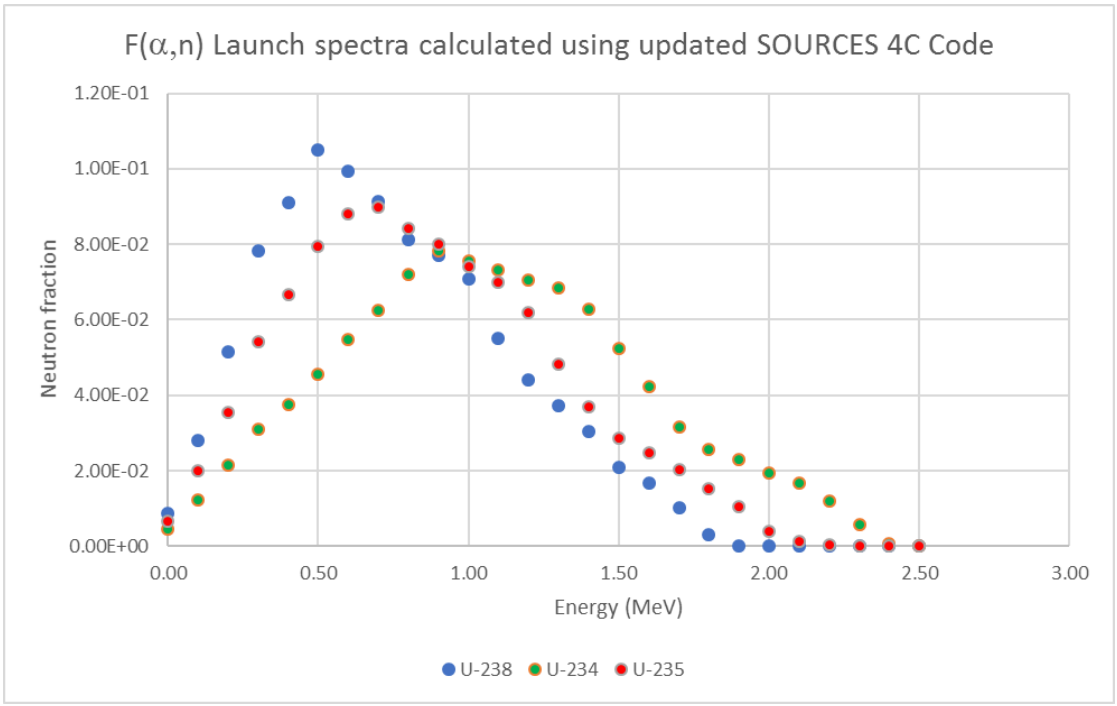

Figure 11. F(α,n) launch spectra for UF_6, calculated using updated SOURCES 4C.

The ^{234}U F(α,n) neutron energy spectrum calculated using the updated SOURCES 4C code was compared with the measured spectra for CaF_2 reported by Jacob and Liskien [15], as show in Figure 12.

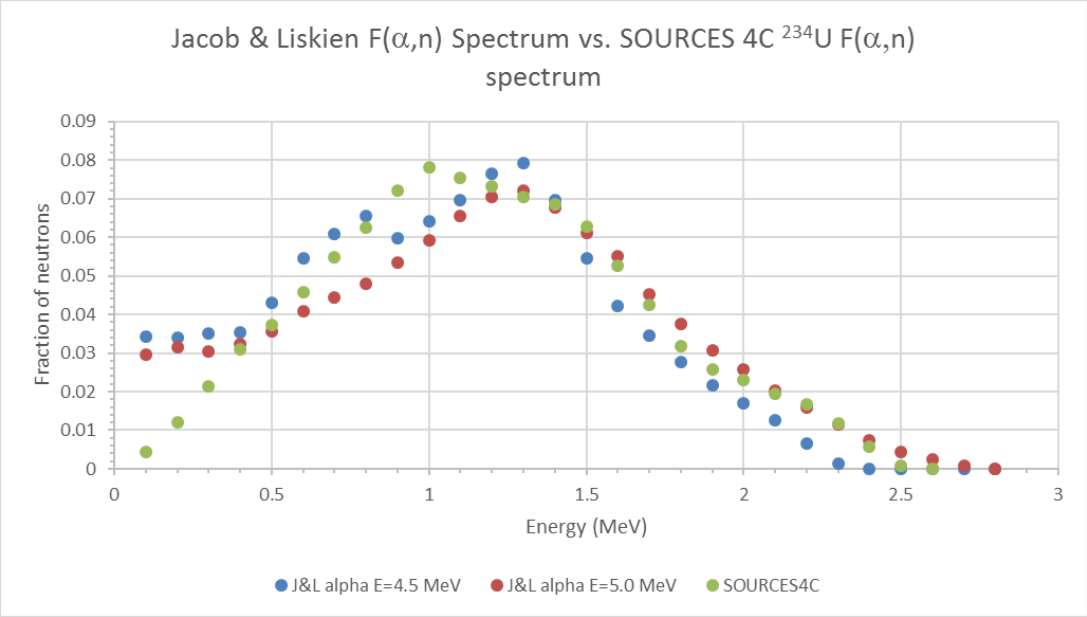

Figure 12. ^{234}U F(α,n) spectrum calculated using updated SOURCES 4C vs measured spectra for CaF_2 [15].

The SOURCES 4C spectrum is bounded by the measured CaF_2 F(α,n) spectra corresponding to alpha energies of 4.5 MeV and 5.0 MeV. It was mentioned earlier that below 0.3 MeV Jacob and Liskien's experimental method has limited analytical power, so a simple flat extrapolation was assumed in all cases. This is evident in Figure 11. One also cannot say with confidence that the SOURCES 4C spectrum is more truthful, since it was calculated based on a blended cross section set. The SOURCES 4C calculations have some shortcomings that need to be addressed as well. For example, the (α,n) spectra are calculated using an assumed isotropic angular distribution in the center-of-mass system. A blended set of microscopic cross sections had to be used since a comprehensive set of thin target microscopic cross sections spanning the entire energy range of interest was not available.

The ^{234}U F(α,n) spectrum from UF_6 calculated using the "initial" (or un-updated) version of SOURCES 4C was compared with the ^{234}U F(α,n) spectrum calculated using the updated version of SOURCES 4C. The results are given in Figure 13, and in Table 3.

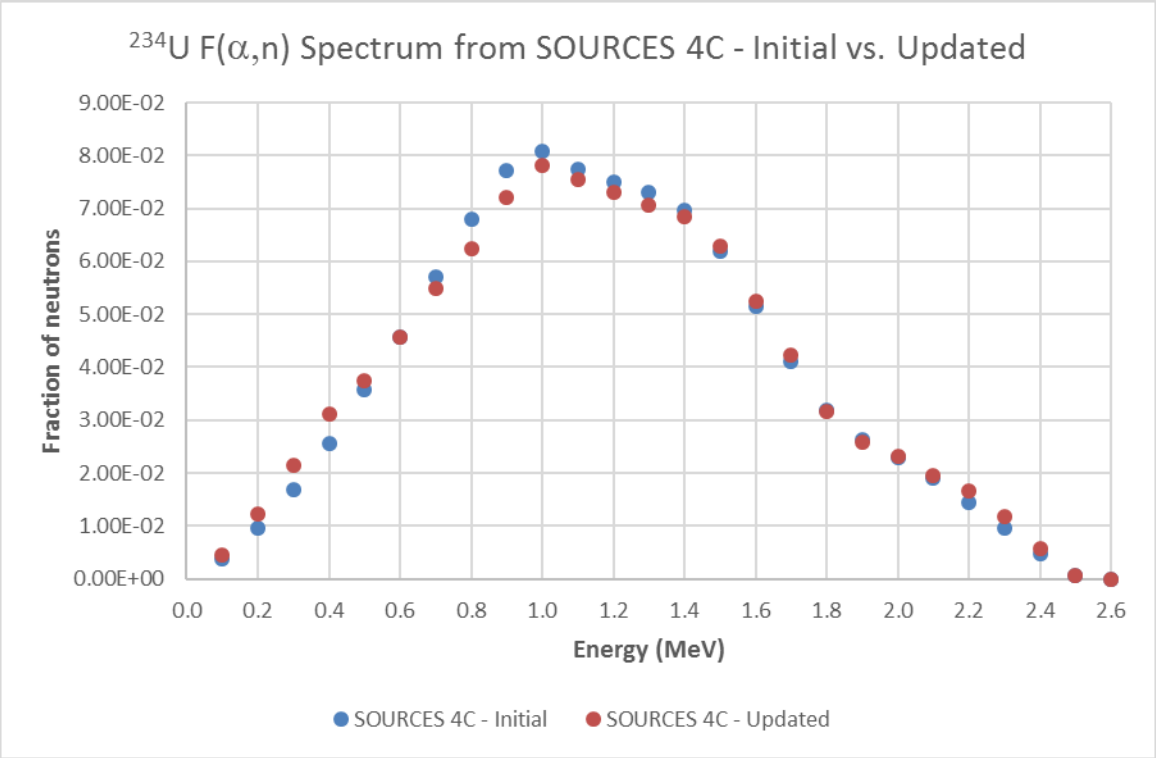

Figure 13. Comparison of ^{234}U F(α,n) spectrum calculated using the initial (un-updated) and updated versions of SOURCES 4C.

Even though the spectra in Figure 13 appear to be close visually, there are differences exceeding 20% between the neutron fractions in some of the energy groups (Table 3).

The average energy of the spectra was very close, however; the initial spectrum was 1.1310 MeV, and the spectrum generated using the updated SOURCES 4C code was 1.1306 MeV.

Efficiency calculations were performed using MCNP and the SOURCES 4C (α,n) spectra for single items, as well as multiple items of the same type counted using the LV-AWCC and the mini-ENMC. The efficiencies for single versus multiple items (e.g., One 1S Monel Cylinder versus Three 1S Monel Cylinders) were very close. Efficiency calculations for single and multiple items (of the same type) were also performed using the ^{238}U spontaneous fission spectrum taken from Terrell and ^{252}Cf spontaneous fission spectrum taken from Mannhart.

Table 3. Ratio of Initial vs. updated ^{234}U F(α,n) Spectra as a function of energy (average of 0.1 MeV wide bins).

Energy (MeV)	Initial/Updated SOURCES 4C
0.05	0.878
0.15	0.789
0.25	0.794
0.35	0.822
0.45	0.954
0.55	1.002
0.65	1.041
0.75	1.089
0.85	1.071
0.95	1.032
1.05	1.027
1.15	1.026
1.25	1.037
1.35	1.019
1.45	0.987
1.55	0.978
1.65	0.971
1.75	1.006
1.85	1.019
1.95	0.995
2.05	0.975
2.15	0.866
2.25	0.815
2.35	0.826
2.45	1.094

As an example, in Figure 14 and Figure 15, we illustrate the MCNP efficiencies for the Hoke cylinder ANL-11, calculated using the ^{234}U F(α,n) spectrum calculated using the updated version of SOURCES 4C. Also shown are the efficiencies corresponding to the measured F(α,n) spectra from Jacob and Liskien [15] at alpha energies of 4.5 MeV and 5.0 MeV. The efficiencies for LV-AWCC and the mini-ENMC are shown for the same item. For both counters, the efficiencies from Jacob and Liskien bound the efficiencies corresponding to UF_6 calculated using updated SOURCES 4C.

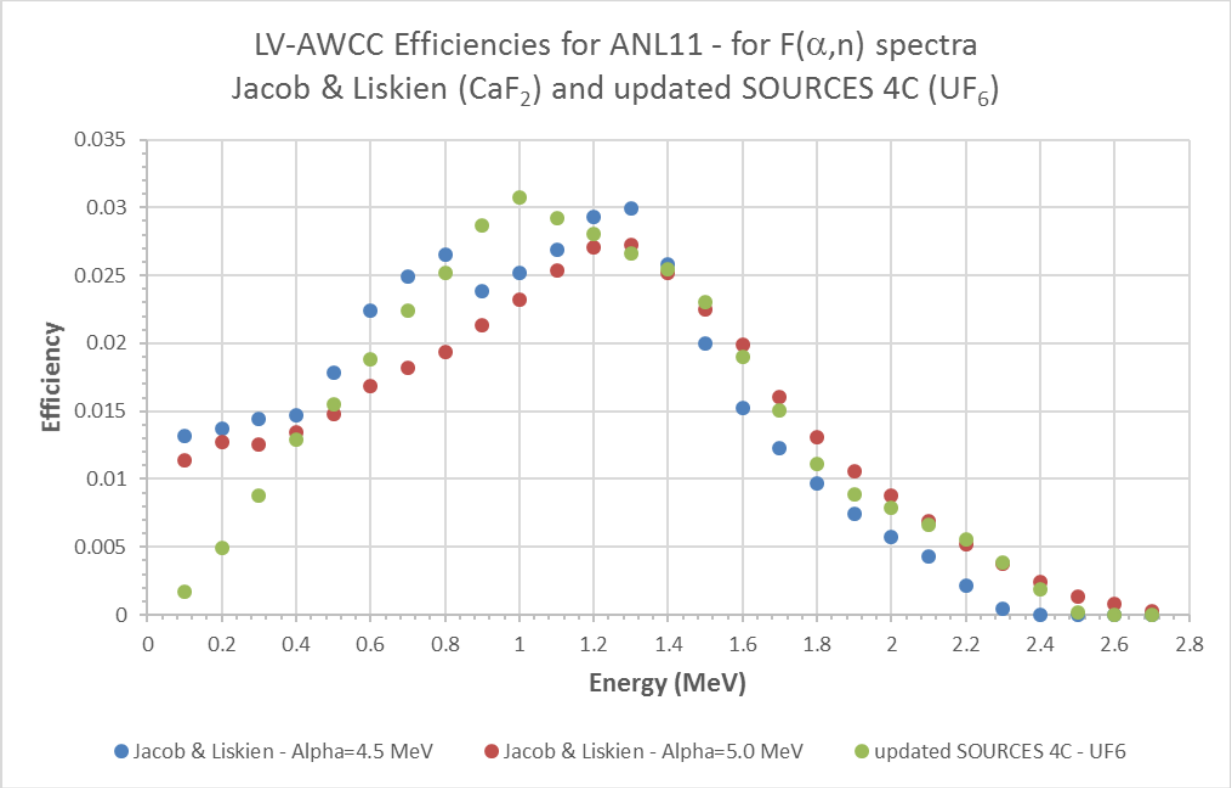

Figure 14. LV-AWCC MCNP efficiencies for UF_6 item Hoke ANL-11, calculated using ^{234}U F(α,n) launch spectrum from updated SOURCES 4C code; also shown are efficiencies using measured F(α,n) spectra from Jacob and Liskien [15], corresponding to alpha energies of 4.5 MeV and 5.0 MeV.

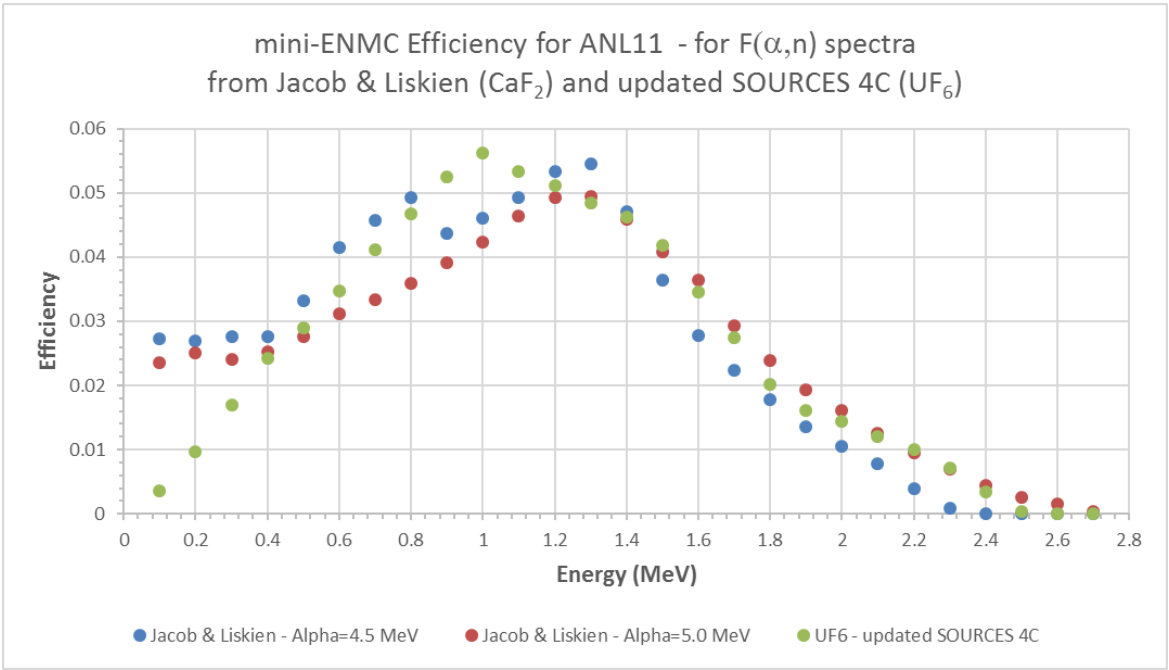

Figure 15. LV-AWCC MCNP efficiencies for UF_6 item Hoke ANL-11, calculated using ^{234}U F(α,n) launch spectrum from updated SOURCES 4C code; also shown are efficiencies using measured F(α,n) spectra from Jacob and Liskien [15], corresponding to alpha energies of 4.5 MeV and 5.0 MeV.

The efficiencies of Hoke ANL-11 UF_6 item are tabulated in Table 4.

Table 4. LV-AWCC and mini-ENMC MCNP efficiencies for Hoke ANL-11 UF_6 item.

F(α,n) Spectrum	LV-AWCC Efficiency (Hoke ANL-11 UF_6 item)	Mini-ENMC Efficiency (Hoke ANL-11 UF_6 item)
^{234}U F(α,n) – SOURCES 4C*	0.3819 ± 0.0002	0.7017 ± 0.0002
CaF_2 - Jacob & Liskien α_E = 4.5 MeV	0.3862 ± 0.0002	0.7143 ± 0.0002
CaF_2 - Jacob & Liskien α_E = 4.5 MeV	0.3803 ± 0.0002	0.7022 ± 0.0002
Avg. of α_E = 4.5 & 5.0 MeV Jacob & Liskien	0.3832 ± 0.0002	0.7082 ± 0.0002

* Using launch spectrum from updated SOURCES 4C.

For the DU item, the ^{238}U(SF,n) correction will be comparatively large as is the (α,n) contribution, so the estimate of (α,n) n/s/g ^{234}U is not well determined from DUF_6. However, one can expect to get a consistent result, albeit within a large estimated experimental uncertainty. Thus, we are compelled to make allowances for the difference in SF and (α,n) spectra for ^{238}U and ^{252}Cf and ^{234}U, respectively.

2.5 TASK 5: DATA REDUCTION AND UNCERTAINTY ANALYSIS

One way to express the deadtime and background corrected net counting rate in terms of detector and measurement item parameters is as follows:

$$C_{net} = (\varepsilon M)_{Cf,meas} \cdot \left(\frac{(\varepsilon M)_{(\alpha,n),mcnp}}{(\varepsilon M)_{Cf,mcnp}}\right) \cdot m_{4eq} \cdot Y_4 + (\varepsilon M)_{Cf,meas} \cdot \left(\frac{(\varepsilon M)_8}{(\varepsilon M)_{Cf}}\right)_{\partial\varepsilon/\partial E} \cdot m_8 \cdot g_8 \cdot \bar{\nu}_{8,tot} \,,$$

where

$(\varepsilon M)_{Cf,meas}$ is the spatially averaged measured efficiency including sample multiplication determined by placing a physically small ^{252}Cf fission source on the surface of the container. The statistical accuracy of measurement is small compared to the systematic uncertainty in our knowledge of the decay-corrected source emission rate, which is about 1.1% at 1σ, based on the NIST $MnSO_4$-bath certificate. The other major consideration is the plausible range of values, depending on where the mobile soild-UF_6 is inside the container. By placing the source at several positions, an uncertainty was assigned based on the spread of the values obtained.

$(\varepsilon M)_{Cf,mcnp}$ is the corresponding calculated value obtained from a detailed Monte Carlo transport simulation using the code MCNP.

$(\varepsilon M)_{(\alpha,n),mcnp}$ is the efficiency multiplication product calculated using MCNP by launching neutrons with the selected $^{234}UF_6$(α,n) spectrum.

m_{4eq} is the ^{234}U equivalent (α,n) mass present in the sample obtained as a weighted sum of all the uranium isotopes, $^{232\text{-}238}$U, present. $m_{4eq} = \sum_{i=2}^{8} \gamma_i \cdot m_i$, where $\gamma_i = {Y_i}/{Y_4}$ is the specific (α,n) neutron yield of ^{23i}U in UF_6 relative to the specific (α,n) neutron yield of ^{234}U in UF_6.

Y_4 is the specific (α,n) neutron yield of ^{234}U in UF_6, the quantity we are interested in.

$\left(\frac{(\varepsilon M)_8}{(\varepsilon M)_{Cf}}\right)_{\partial\varepsilon/\partial E}$ is the ratio of the efficiency multiplication product for ^{238}U(SF,n) neutrons relative to that for ^{252}Cf(SF,n) neutrons, with the subscript $\partial\varepsilon/\partial E$ denoting that the numerical value of this ratio may be determined from the known slope of the efficiency curve of the detector as a function of mean spectrum energy. For the present analysis, including delayed neutrons, we take the mean energy of the ^{252}Cf system to be 2.126 MeV, and from systematics, the corresponding value for ^{238}U is estimated as 1.849 MeV. Assigning ±50 keV uncertainty in each, the difference is 277±71 keV. On this basis from previous experiments and calculations, respectively, we estimate $\left(\frac{(\varepsilon M)_8}{(\varepsilon M)_{Cf}}\right)_{\partial\varepsilon/\partial E}$ to be (1.0317±0.0081) for the ORNL LV AWCC using the JCC-51 as an analog. This treatment assumes that the multiplication is similar for both prompt fission neutron spectrum–dominated systems, which seems reasonable given that the multiplication is also close to unity for all items. A more refined analysis is possible but not needed for the HEU items reported here for which the ^{238}U correction is small.

m_8 is the mass of ^{238}U, g_8 the specific spontaneous fission rate of ^{238}U, and $\bar{\nu}_{8,tot}$ the average total (prompt + delayed) number of neutrons emitted following spontaneous fission of ^{238}U [16]. The product of $g_8 \cdot \bar{\nu}_{8,tot}$ is the specific SF total neutron yield and is known from evaluated nuclear data. For the present analysis we take the value of (0.01334±0.00023) n/s/g. Note that on a per-gram basis the neutron generation rate from ^{234}U is over four orders of magnitude greater, and so it is easy to see that for HEU with ^{234}U present at about 1 wt% and ^{238}U present at about 9 wt%, the ^{238}U subtraction is a minor correction.

The definition of m_{4eq} provides a convenient way to correct for the (α,n) contribution for uranium isotopes other than ^{234}U. Fortunately for this, only the relative shape of the UF_6(α,n) yield curve is needed over a narrow energy range. For our initial analysis, we adopted the γ_i estimates of Croft [11]. Thus, explicitly we have

$$m_{4eq} = 6707 \cdot m_2 + 1.655 \cdot m_3 + m_4 + 0.0001934 \cdot m_5 + 0.006745 \cdot m_6 + 0.00001992 \cdot m_8 \ .$$

We note that the γ-value for ^{232}U is for pure (fresh) ^{232}U. For aged uranium in which the ^{232}U is in secular equilibrium with its decay chain, the value is roughly an order of magnitude higher. Fortunately, ^{232}U is completely absent or present only in trace amounts in our items, and so the impact is negligible. Similarly, the amount of ^{233}U in our items also has an inconsequential impact on the (α,n) production rate. Note that in the present treatment we are neglecting the spectral difference between ^{234}U, ^{235}U, and ^{238}U generated F(α,n) neutrons, which is justified for the HEU items because the effect is small and the deviation of m_{4eq} from m_4 is at most 2.8 %. Subsequently we updated the m_{4eq} correction using our blended cross section scaled to recreate thick-target ^{234}U yield using stopping power calculated from SRIM 2013. We also allowed for relative differences in detector efficiency of (α,n) for different sources. The impact was modest.

Although the ratio $\left(\frac{(\varepsilon M)_{(\alpha,n),mcnp}}{(\varepsilon M)_{Cf,mcnp}}\right)$ is calculated for each item, the numerical value varies only slightly between them. This allows us to make some rather general statements about the uncertainty structure.

For the UF_6(α,n) spectrum we took the time-of-flight histograms with 0.1 MeV wide energy bins, reported by Jacobs and Liskien [15], which were measured by bombarding thick CaF_2 targets with α-particle beams. We took the spectrum for 4.5 MeV incident energy to be too soft, with a mean energy of about 0.999±0.04 MeV, and the spectrum for 5.0 MeV incident energy to be too hard, with a mean energy of about (1.122±0.05) MeV. As our best estimate we adopted the average of the two (the yield weighted mean α-energy is about 4.76 MeV, close to that of ^{234}U) and assigned an uncertainty based on half the difference. The statistical precision (Monte Carlo sampling error) was less than 0.042% relative standard deviation (rsd) in all cases. The uncertainty assigned to spectrum uncertainty was much larger, at 0.78 % rsd.

For the ^{252}Cf(SF,n) prompt fission neutron spectrum, we adopted the evaluation of Mannhart. Sampling precision was approximately 0.031% rsd in all cases. The systematic uncertainty associated with the uncertainty in the shape of the spectrum was estimated by propagating the full covariance matrix generated by Mannhart for the 71 energy-group representation. Mannhart's spectrum and covariance matrix were taken from ENDF/B-VII.1, and the evaluation is described in the references. The resulting uncertainty was less than or about 0.084 % rsd in all cases and therefore represents a systematic error.

The modelling uncertainty inherent in the Monte Carlo calculation of the ratio $\left(\frac{(\varepsilon M)_{(\alpha,n),mcnp}}{(\varepsilon M)_{Cf,mcnp}}\right)$ is far more difficult to assess. It depends on details of neutron interaction cross sections and thermal scattering

kernels, which are mainly unquantified in the data libraries yet transcend gross geometrical, material, and density representations that can be studied by brute force difference calculations. We note, however, that even on an absolute basis the agreement between the measured and MCNP-calculated efficiency multiplication product for ^{252}Cf is excellent. The relative differences are better than 0.3%, which is far better than how well we know the ^{252}Cf emission rate used to make the measurements. Our expectation is that neutron transport model bias will be both minimized and reduced to a relatively minor contributor to the overall uncertainty by forming the ratio, although (α,n) and fission spectra do of course sample the energy response of the detector differently, especially in the higher neutron energies (as opposed to the thermal region). However, we are fully aware that this assumption should be tested and subjected to critical thinking as more sophisticated tools and data sets become available in order to avoid the potential pitfalls of modeling [26].

Rearranging the response expression, we obtain the following measurement equation for Y_4:

$$Y_4 = \frac{\frac{C_{net}}{(\varepsilon M)_{Cf,meas}} - \left(\frac{(\varepsilon M)_8}{(\varepsilon M)_{Cf}}\right)_{\partial\varepsilon/\partial E} \cdot m_8 \cdot (g_8 \cdot \bar{\nu}_{8,tot})}{\left(\frac{(\varepsilon M)_{(\alpha,n),mcnp}}{(\varepsilon M)_{Cf,mcnp}}\right) \cdot m_{4eq}} \quad . \tag{3}$$

In Table 4 we present results for several of our UF_6 items measured singly in the LV AWCC during the first two campaigns. Note we have three isotopic compositions, two types of cylinders, and seven items. Although all the items are HEU with about 90.1 atom% enrichment in ^{235}U they differ markedly in ^{234}U content. Also note the P-10's were filled from the corresponding Hoke containers and so any decay product impurities would be left behind, but we do not see any change in specific emission rate. Also shown is the number of times, N, each item was measured. Each time represents a repositioning of the item and reassessment of the ambient background.

The results for HEU items that were measured in this work are summarized in Table 5. The data set consists of UF_6 items of at least three different ^{234}U abundances, measured (multiple trials in some cases) using two different neutron counters and over three different measurement campaigns spanning several months. ***The unweighted mean of the neutron yield from ^{234}U ^{19}F(α,n) is 508.2 n/s/g ^{234}U, with a relative standard deviation of ± 8.2 n/s/g ^{234}U (a relative standard deviation of ± 1.6%). The less than 2% relative standard deviation is indicative of the robustness of the measurements and the analysis. The weighted mean of the neutron yield is 509.5 ± 1.3 n/s/g ^{234}U (or ± 0.25% uncertainty).***

Table 5. Summary of Results for HEU items.

S.No.	Measurement Item	^{235}U (at%)	^{234}U (at%)	Trials (N)	Counter	Y -^{234}U (n/s/g)	σ_Y (n/s/g)	% Unc.
1	ANL-10 Hoke	90.1	0.871	3	LV AWCC	506.8	4.4	0.9
2	ANL-10 P10-2	90.1	0.871	1	LV AWCC	510.1	6.8	1.3
3	ANL-10 P10-2	90.1	0.871	2	mini-ENMC	489.7	14.9	3.1
4	ANL-10 P10-3	90.1	0.871	1	LV AWCC	505.4	4.9	1.0
5	ANL-10 P10-3	90.1	0.871	2	mini-ENMC	507.3	7.1	1.4
6	ANL-10 P10-2&3	90.1	0.871	1	LV AWCC	515.4	4.7	0.9
7	ANL-10 P10-2&3	90.1	0.871	1	mini-ENMC	506.4	6.5	1.3
8	ANL-11 Hoke	90.1	1.40	3	LV AWCC	511.7	4.2	0.8
9	ANL-11 Hoke	90.1	1.40	1	LV AWCC	517.8	15.1	2.9
10	ANL-11 Hoke	90.1	1.40	2	mini-ENMC	517.4	3.9	0.8
11	ANL-10&11&12 Hoke	90.2	2.19	3	LV AWCC	505.8	4.2	0.8
12	ANL-10&11&12 Hoke	90.2	2.19	2	LV AWCC	510.1	6.8	1.3
13	ANL-10&11&12 Hoke	90.2	2.19	3	mini-ENMC	511.6	5.6	1.1
14	ANL-10&11&12 Hoke	90.2	2.19	2	LV AWCC	505.4	4.9	1.0
15	ANL-10&11&12 Hoke	90.2	2.19	2	mini-ENMC	504.7	11.6	2.3
16	ANL-10&11&12 Hoke	90.2	2.19	1	LV AWCC	491.6	5.1	1.0
17	ANL-10&11&12 Hoke	90.2	2.19	1	mini-ENMC	522.8	5.6	1.1
18	ANL-10&11&12 Hoke	90.1	1.49	1	LV AWCC	507.0	5.7	1.1

The reported statistical uncertainty at approximately 68% confidence represents an attempt to accurately capture all sources of random variability (including source migration inside the containers with time). Systematic uncertainty is dominant and is about the same for the measurements in both counters. Taking the analysis of ANL-11 Hoke item as an example, the uncertainty budget for the ^{234}U F(α,n) neutron yield from UF_6 is listed in Table 6.

Cf-252 source strength	1.1%	NIST certificate uncertainty
alpha-n spectrum	0.9%	Jacob & Liskien sensitivity study
Cf-252 spectrum	0.1%	Mannhart full covariance analysis
MCNP model and cross section bias	0%	assumed negligible in the ratio calculation

Positional uncertainties are automatically taken into account case by case in the analysis and contribute in the spread of the results when items are measured repeatedly within a campaign and across campaigns with the same or different detectors.

It is not our intention here to provide a detailed review of the literature or make a comprehensive comparison to other works, but we note that a commonly used value in nuclear safeguards is that recommended by Sampson [27] of 576±42 n/s/g ^{234}U in UF_6. Recently two estimates based on field measurements of collections of large commercial storage at enrichment plants have been reported [28]. Miller et al. [7] found a value of 474±21 n/s/g ^{234}U was consistent their observations, while Kulisek et al. [8] gives a value of 503 n/s/g ^{234}U derived from 219 cylinders ranging from natural to 5 wt% of known ^{234}U abundance. The standard deviation across the measurements (excluding clear outliers) is 2.6%. Benchmarking of the Monte Carlo model using ^{252}Cf is good to about 2%. It is hard to estimate other uncertainty contributions including the allowance for non-^{234}U α-induced neutrons, which depends on enrichment. However, an overall uncertainty on the order of 4% at 1-σ would seem plausible based on the description of the measurements. We consider the agreement between the field data and our laboratory-based measurements to be extremely good.

In addition to HEU items, LEU items and a DU item were also measured. Table 6 gives the results from the LEU items IS Monel, NBL-22, and NBL-7, and the DU item.

Table 6. Results summary for LEU and DU UF_6 items.

S.No.	Measurement Item	^{235}U (at%)	^{234}U at%	Trials (N)	Counter	Y -^{234}U (n/s/g)	σ_Y (n/s/g)	% Unc.
1	Pedigree 1S 1	4.62	0.0193	3	mini-ENMC	539.3	9.5	1.8
2	Pedigree 1S 2	4.62	0.0193	3	mini-ENMC	527.5	9.3	1.8
3	Pedigree 1S 3	4.62	0.0193	1	LV AWCC	521.6	8.3	1.6
4	Pedigree 1S 3	4.62	0.0193	2	LV AWCC	539.6	8.6	1.6
5	Pedigree 1S 3	4.62	0.0193	3	mini-ENMC	530.0	9.2	1.7
6	Pedigree 1S 2&3	4.62	0.0193	3	mini-ENMC	554.3	10.8	1.9
7	Pedigree 1S 1&2&3	4.62	0.0193	1	LV AWCC	512.8	9.3	1.8
8	Pedigree 1S 1&2&3	4.62	0.0193	3	mini-ENMC	533.2	11.2	2.1
9	NBL-22 2S	4.61	0.0192	2	LV AWCC	460.0	9.0	1.9
10	NBL-22 2S	4.61	0.0192	3	mini-ENMC	462.2	9.2	2.0
11	NBL-22 2S	2.73	0.0211	3	mini-ENMC	493.2	8.6	1.8
12	DU keg	0.291	0.00133	3	mini-ENMC	901.2	61.8	6.9

In Table 6, the average neutron yield from the 1S items is greater than the weighted mean value from the HEU items by approximately 4.5%. One possible reason for the systematically high value of the neutron yield could be the contribution from the spontaneous fission of ^{238}U, as well as ^{238}U F(α,n) neutrons. A correction factor is being calculated to account for these contributions. The neutron yield from the LEU item NBL-7 is within 2σ of the uncertainties with respect to the yield from the HEU items, but the results for the NBL-22 LEU items is biased low by 9.4%. The reason for this bias is being investigated. The ^{234}U $^{19}F(\alpha,n)$ neutron yield result for the DU keg is clearly an outlier when compared with the HEU and LEU results. We are investigating the reasons for this significant positive bias.

2.6 TASK 6: COLLABORATE WITH LANL IN CREATING PRESENTATIONS, GENERATING PUBLICATIONS, AND IN COMMUNICATION AND ARCHIVING OF RESULTS

A paper titled "The Specific (α,n) Production Rate for ^{234}U in UF_6" was presented at the SORMA conference held in Ann Arbor from June 11–14, 2018. After a peer review, the paper was published the journal *Nuclear Instruments and Methods in Physics Research A*.

Additionally, a paper titled "Status of (α,n)-reaction data for nuclear safeguards" was presented at the INMM 2018 conference and was published in the proceedings. The authors of both the papers are Stephen Croft (ORNL), Andrea Favalli (LANL), Glenn Fugate (ORNL), Robert McElroy (ORNL), Angela Simone (University of Tennessee), Martyn Swinhoe (LANL), and Ramkumar Venkataraman (ORNL).

Besides collaboration on these publications, ORNL and LANL scientists worked closely developing the MCNP models of UF_6 item geometries for efficiency calculations, planning and performing measurements using the mini-ENMC neutron counter, and discussing the results obtained.

2.7 TASK 7: THOROUGH DOCUMENTATION AND REPORTING OF THE DELIVERABLES—PROVIDE QUARTERLY REPORTS AND END-OF-YEAR REPORT

Quarterly reports were provided for all quarters of FY 2018, and for the first two quarters of FY 2019. A one page summary was prepared for inclusion in NA-22 Annual Report. An end-of-the-year report will be provided, capturing all the work that was performed and the deliverables.

2.8 TASK 8 (LANL): PERFORM MEASUREMENTS USING THE LANL ENMC AND THE SAME UF_6 SOURCES THAT WERE MEASURED WITH LV-AWCC. THE LANL ENMC WILL BE SHIPPED TO ORNL. LANL PHYSICIST ANDREA FAVALLI WILL SET UP AND PERFORM MEASUREMENTS AT ORNL. THE MEASUREMENTS WILL BE

USED TO DIRECTLY DETERMINE THE SPECIFIC NEUTRON YIELD (NEUTRONS/SEC/GRAM) OF ^{234}U.

The mini-ENMC was shipped from LANL to ORNL in Q2 of FY 2018. LANL scientist Dr. Andrea Favalli visited ORNL in January 2018 and participated in measurements of UF_6 items using the mini-ENMC. All the UF_6 items that were counted using the LV-AWCC were also counted using the mini-ENMC. The MCNP model of the mini-ENMC was updated to include the UF_6 item geometries of interest. All the MCNP efficiency calculations were performed using the mini-ENMC model as well. Data reduction was performed.

2.9 ADDITIONAL TASK

The methods and concepts developed in this work can be applied to investigating other (α,n) reactions that are of interest in nuclear safeguards applications, e.g., O (α,n). The PI on the current project, Dr. Stephen Croft, has supported the work done on O(α,n) reaction [29], [30], [31], [32].

3. CONCLUSIONS

The purpose of our measurements was to support a science-based approach by measuring the specific (α,n) yield in neutrons per second per gram of ^{234}U in UF_6. To do this, two recognized safeguards instruments— the LANL Mini-ENMC and the ORNL LV AWCC—were used to measure a diverse collection of well-characterized small samples. The instruments are efficiency calibrated using a National Institutes of Standards and Technology (NIST)–certified ^{252}Cf source. A Monte Carlo transport code (MCNP)–based adjustment to the F(α,n) launch spectrum and items was made using spectra taken from the literature as well as those predicted by the SOURCES4C code. Efficiency calculations using MCNP were completed for a variety of UF_6 items in the LV-AWCC and the LANL mini-ENMC counters. The efficiencies from MCNP were compared against measured efficiencies using the NIST-calibrated ^{252}Cf source FTC-1830. An agreement of better than a few tenths of a percent was obtained. The efficiency for (α,n) neutrons was then obtained by multiplying this by the ratio of (α,n) to ^{252}Cf efficiencies (calculated using MCNP). For the MCNP calculations, the evaluated ^{252}Cf fission spectrum of Mannhart was used. This is available in 71 groups and has a full covariance matrix. The systematic uncertainty associated with the uncertainty in the shape of the spectrum was estimated by propagating the full covariance matrix generated by Mannhart for the 71 energy-group representation. The code SOURCES 4C was used to predict the (α,n) energy spectrum. The SOURCES 4C code makes use of thin target data, a nuclear model for energetics, and stopping power data. SOURCES 4C was updated for this case alone, namely,^{234}U ^{19}F(α,n) yields from UF_6. The alpha stopping powers were calculated using the code SRIM, and

coefficients of the polynomial fits were calculated. SOURCES 4C code was updated using the alpha stopping powers and the microscopic cross sections available to ORNL from a previous NA-22 project. In this project we built-in benchmarks based on measurements we took, or measurements available in the literature, in order to validate calculations (MCNP and other). The weighted mean of the neutron yield, based on the HEU items that were measured, is 509.5 ± 1.3 n/s/g ^{234}U (or ± 0.25% uncertainty). The uncertainty in the weighted mean does not include systematic uncertainties. For HEU items, the dominant sources of uncertainty are efficiency determination, approximately 0.9% relative standard deviation, associated with the ^{252}Cf reference source and an additional about 1.1% systematic uncertainty coming from the uncertainty in the F(α,n) spectrum. For the 1S Cylinder LEU items that were measured (4.6% ^{235}U abundance), the ^{234}U F(α,n) yields are 4.5% higher on average when compared with the yield from the HEU item. For the NBL22 LEU items, which are also 4.6% enriched in ^{235}U, the ^{234}U F(α,n) yields are biased low by about 9.4% with respect to the yield from the HEU item. The yield averaged over the results from the two sets of items, both 4.6% enriched, is 496 n/s/g. The reason for the spread is not known. The result for the DU item is high by 40%. This is clearly an outlier compared to the HEU and LEU results. Indications are, based on neutron coincidence counting, that the book value for the mass is understated. We are investigating the reasons for these biases and will apply appropriate corrections. The updated SOURCES 4C code is available to the safeguards community and beyond from the Radiation Safety Information Computational Center (RSICC) at ORNL, which is a repository for computer codes used in the field of nuclear technology. The ^{234}U ^{19}F(α,n) yield from UF_6 established in this project will be shared with the NDA Working Groups associated with the Institute of Nuclear Material Management (INMM) and the European Safeguards Research and Development Association (ESARDA). The updated yield and the publications related to this work will be included in the next revision of the relevant ASTM C26.10 and ANSI N15 standards.

4. FUTURE WORK

Accurate (α,n) yields and spectra of actinide compounds are required to support a range of different applications including basic nuclear physics, neutron background and activation estimation, nuclear waste characterization, dosimetry and health physics, nondestructive mass assay of fresh and used nuclear fuel, nuclear safeguards, and materials control and accountancy. From an applications perspective, the thick-target integrated over angle yield curve is perhaps the most important function. This can be measured directly using continuous α-beams using a flat (efficiency in energy) 4π neutron detector or via associated activation techniques where applicable. Alternatively, it can be calculated from a thin target (microscopic data). Except in the case of UO_2, trusted measurements have *not* been made on actinide compounds of

interest but are made on other materials. Often the detection systems deployed do not provide as complete a coverage as one would like. Scaling between materials incurs an additional error that needs to be quantified, especially with regard to stopping powers and the Bragg-Kleeman mixing rule. The experimental data generally show scatter that is far greater than claimed by the reporting researchers. This could be in part due to unrecognized bias arising from changing detection efficiency as the α-energy sweeps over thresholds and resonances. A concerted experimental effort is needed to resolve the discrepancies in the literature; otherwise, performing meaningful first-of-a-kind data evaluations for charged particle reactions for technological applications is seriously hampered. High-quality benchmark and comparison data of high accuracy are also needed to validate and, in some cases, normalize accelerator measurements. Knowledge of emitted neutron energy spectra is especially patchy yet much needed. Calculations rely on differential partial cross sections which are difficult to determine and cannot be calculated from first principles with present tools to the required accuracy. Pulse beam time-of-flight measurements as a function of angle off thick targets are therefore recommended as the first step. Again, complementary measurements on stable homogenous actinide compounds using a variety of spectrometers are needed for purposes of validation.

5. REFERENCES

1. GS Solov'ev, AV Saprygin, VV Komarov, and AI Izrailevich, ^{234}U content in enriched uranium as a function of the ^{234}U concentration in the initial material, *Atomic Energy* 95(1) (2003) 473-475. Translated from *Atomnaya Énergiya* 95(1) (July 2003) 32-34.

2. KD Kimball, *Recommendations of ^{235}U/^{234}U ratios and alpha-neutron yields for the K-25/K-27 D&D neutron NDA methodology*, Bechtel Jacobs Company/Oak Ridge report BJC/OR-2862, Rev 0 (August 2007).

3. D Grady, E Smith, K Chand, M Swinhoe, and J Kulisek, *U-235/U-234 ratio behavior in gas centrifuge enrichment plants and implications for unattended verification of UF6 cylinders by safeguards inspectorates*, Lawrence Livermore National Laboratory report LLNL-TR-739009 (September 2017) Official Use Only.

4. AM Shephard, BR Thomas, JB Coble and HG Wood, "Minor isotope safeguards techniques (MIST): Analysis and visualization of gas centrifuge enrichment plant process data using the MSTAR model," *Nucl. Instrum. Meths. Phys. Res*. A890 (2018) 79-83.

5. Z Zarpas, A Lorber, H Sela, O Paz-Tal, Y Hagag, P Kurttio, and L Salonen, "Measurement of the 234U/238U ratio by MC-ICPMS in drinking water, hair, nails, and urine as an indicator of urine exposure source," *Health Physics* 89(4) (2005) 315-321.

6. RB Walton, TD Reilly, JL Parker, JH Menzel, ED Marshall, and LW Fields, Measurements of UF_6 cylinders with portable instruments, *Nuclear Technology* 21(February 1974)133-148. These authors use a value of 460 n/s/g 234U and relative yield per alpha factors of 0.56, 0.75 and 0.38 for ^{235}U, ^{236}U and ^{238}U, respectively. The reference for these values is TD Reilly, JL Parker, AE Evans, and RB Walton, "Uranium enrichment measurements on UF_6 product cylinders," in *Nuclear Safeguards Research and Development Progress Report May-August 1971*, Los Alamos Scientific Laboratory report LA-4794-MS(1971)16-19. These authors determined experimentally the $UF_6(\alpha,n)$ n/s/g ^{234}U by counting with a neutron slab detector the emission of three type 5A cylinders of differing ^{234}U enrichment (0.10, 0.52, and 0.75 %). Few details are provided, and no uncertainty analysis is provided, although an allowance for self-multiplication was made. The relative yield per alpha factors seems to have been based on data taken from E Amaldi, *Handbook der Physik*, Vol. XXXVIII/2, p.109. Note Reilly et al. credit JL Feuerbacher with the original concept of total neutron counting to assay bulk UF_6.

7. KA Miller, MT Swinhoe, S Croft, T Tamura, S Aiuchi, and T Iwamoto, "Measured F(α,n) Yield from ^{234}U in Uranium Hexafluoride," Nuclear Science and Engineering 176(2014)98-105.

8. JA Kulisek, BS McDonald, LE Smith, MA Zalavadia, and JB Webster, "Analysis of indirect neutron signature for enhanced UF_6 cylinder verification," Nucl. Instrum. and Meths. in Phys. Res A846 (2017) 36-42.

9. LE Smith, AR Lebrun, and R Labella, Unattended safeguards instrumentation at centrifuge enrichment plants, ESARDA Bulletin 51 (December 2014) 58-66. ISSN 0392-3029. https://esarda.jrc.ec.europa.eu.

10. AM LaFleur, S Croft, RL Mayer, MT Swinhoe, DR Mayo, and BA Sapp, "Traceable determination of the absolute neutron emission yields of UO2F2working reference materials," 2013 3rd International Conference on Advancements in Nuclear Instrumentation, Measurement Methods and their Applications (ANIMMA), Marseille, 2013, pp. 1-8.

11. S Croft, "The thick target (α,n) yield of fluorine compounds for a broad range of actinides," 19th Annual ESARDA (European Safeguards Research and Development Association) Symposium on Safeguards and Nuclear Material Management, Montpellier, France, May 13-15, 1997. ESARDA 28 EUR 17665 EN(1997) 397-404.

12. WB. Wilson, RT. Perry, JE Stewart, TR England, DG Madland, and ED Arthur, "Development of the SOURCES code and data library for the calculation of neutron sources and spectra from (α,n) reactions, spontaneous fission, and β- delayed neutrons," *Applied Nuclear Data Research and Development Semiannual Progress Report Oct. 1, 1982 – Mar. 31, 1983*, compiled by E.D. Arthur: Los Alamos Report LA-9841-PR (Aug., 1983)65-66 with references on p84.

See also:

WB Wilson, JE Stewart, and RT Perry, *The $^{19}F(\alpha,n)$ neutron production from the decay of U nuclides in UF_6, Los Alamos Scientific Laboratory Applied Nuclear Data Research and Development Progress Report for the Period October 1 – December 31, 1980*, complied by CI Baxman and PG Young. Report LA-8757-PR (March 1981) 40-52.

RT Perry and WB Wilson, *Neutron Production from (α,n) Reactions and Spontaneous Fission in ThO_2, UO_2, and $(U,Pu)O_2$ Fuels*, Los Alamos National Laboratory report LA-8869-MS (June 1981).

WB Wilson, JE Stewart and RT Perry, "Neutron Production in UF_6 from the Decay of Uranium Nuclides," *Transactions of the American Nuclear Society* 38(1981)176.

W.B Wilson and RT Perry, Thick-Target Neutron Yields in Boron and Fluorine, Los Alamos National Laboratory memorandum T-2-M-1835 to N. Ensslin (1987).

IC Gauld, EF Shores, and RT Perry, "New neutron source algorithms in the ORIGEN-S code," paper presented at American Nuclear Society/Radiation Protection & Shielding Division, 12th Biennial RPSD Topical Meeting, April 14-18, 2002, Santa Fe, New Mexico.

13. H Menlove, *Description and Operation Manual for the Active Well Coincidence Counter*, Los Alamos National Laboratory, report LA-7823-M, Los Alamos National Laboratory, Los Alamos, NM, 1979.

14. W. Mannhart, "Evaluation of the Cf-252 fission neutron spectrum between 0 MeV and 20 MeV," in *Properties of Neutron Sources*, IAEA TECDOC-410(Vienna, March 1987)158-171.

15. GJH Jacobs and H Liskien, "Energy Spectra of Neutrons Produced by α-Particles in Thick Targets of Light Elements," *Annals of Nuclear Energy* 10(10) (1983) 541-552.

See also:

W Mannhart, "Status of the Cf-252 fission-neutron spectrum evaluation with regard to recent experiments," in *Physics of Neutron Emission in Fission*, HD Lemmel (Editor), IAEA INDC(NDS)-220 (June 1989) 305-336.

W Mannhart, "Data fitting and evaluation techniques for neutron spectra," in *International Symposium on Nuclear Data Evaluation Methodology*, C.L. Dunford (Editor), World Scientific Publishing Co. Pte. Ltd. (1993) 247-256. ISBN 981-02-1285-2.

J Terrell, "Prompt neutrons from fission," Proc. Symp. Phys. & Chem. of fission, Salzburg, IAEA, Vienna, Vol. 2 (1965) 3-24.

16. J Campbell and G Spriggs, "Recommended relative abundances and energy spectra for the eight time-group representation," Appendix 3 of *Delayed neutron data for the major actinides*, a report by the working party of international evaluation co-operation of the NEA nuclear science committee, NEA OECD report NEA/WPEC-6(2002).

17. V Benji and D Mostacci, "Neutrons from (α,n) reactions in uranium hexafluoride," *Applied Radiation and Isotopes* 48(2) (1997) 213-214.

18. ZW Bell, K-P Ziock, MF Ohmes, Y Xu, T Downar, and SA Pozzi, "Measurement of neutron yields from UF_4," *IEEE Trans on Nucl Sci* 57(4) (August, 2010) 2239-2246.

19. W.A. Peters et al., *A kinematically complete interdisciplinary and co-institutional measurement of the $^{19}F(\alpha,n)$ cross section for nuclear safeguards science*, Idaho National Laboratory Report INL/EXT-16-38791.

20. JF Ziegler, JP Biersack, and MD Ziegler, SRIM The Stopping and Range of Ions in Matter (SRIM Co., 2008) ISBN-13: 978-0-9654207-1-6, available from www.SRIM.org.

21. M Balakrishnan, S Kailas, and MK Mehta, "A study of the reaction $^{19}F(\alpha,n)^{22}Na$ in the bombarding energy range 2.6 to 5.1 MeV," *Pramāna* 10(3) (1978) 329-339.

22. PR Wrean and RW Kavanagh, "Total cross sections and reaction rates for $^{19}F(\alpha,n)^{22}Na$, $^{22}Ne(p,n)^{22}Na$, and their inverses," *Phys. Rev*. C62, 055805 (2000). See also PR Wrea, $^{19}F(\alpha,n)^{22}Na$, $^{22}Ne(p,n)^{22}Na$, and the role of their inverses in the destruction of ^{22}Na, PhD Dissertation, California Institute of Technology, Pasadena, California, USA (1998).

23. EB Norman, TE Chupp, KT Lesko, PJ Grant, and GE Woodruff, "^{22}Na Production Cross Sections from the $^{19}F(\alpha, n)$ Reaction," *Phys. Rev*. C 30, 1339 (1984).

24. EB Norman, TE Chupp, KT Lesko, PJ Grant, and GE Woodruff, "$^{19}F(\alpha,n)$ thick target yield from 3.5 to 10.0 MeV," *Applied Radiation and Isotopes* 103 (2015)177-178.

25. S Croft, "The thick target (α,n) yield of fluorine compounds for a broad range of actinides," 19th Annual ESARDA (European Safeguards Research and Development Association) Symposium on Safeguards and Nuclear Material Management, Montpellier, France, May 13-15, 1997. ESARDA 28 EUR 17665 EN(1997)397-404.

26. HG Huges, "Uncertainties beyond statistics in Monte Carlo simulations," *Radiation Protection Dosimetry* 126(1-4) (2007) 45-51.

27. TE Sampson, "Neutron yields from uranium isotopes in uranium hexafluoride," *Nucl Sci & Engin* 54(4) (1974) 470-474.

28. GC-Y. Chan, JD Valentine, and RE Russo, Towards novel field-deployable instrumentation for UF6 enrichment – an overview of existing and emerging technologies, ESARDA Bulletin 54 (June 2017) 31-43. ISSN 0392-3029. https://esarda.jrc.ec.europa.eu.

29. MT Pigni, S Croft, and IC Gauld, "Uncertainty quantification in (α,n) neutron source calculations in an oxide matrix," *Progress in Nuclear Energy* 147 (2016) 147-152.

30. MT Pigni, IC Gauld, and S Croft, "Early applications of the R-matrix SAMMY code for charged-particle induced reactions and related covariances," EPJ Web of Conferences 146 (2017) 02019.

31. MT Pigni, S Croft, and IC Gauld, “Uncertainty quantification in (α,n) neutron source calculations in an oxide matrix,” IAEA Consultants’ Meeting on R-Matrix Codes for Charged-Particle Reactions in the Resolved Resonance Region (RRR) held at the International Atomic Energy Agency (IAEA) Headquarters, Vienna, Austria (December 5-7, 2016).

32. MT Pigni, IC Gauld, and S Croft, “Intrinsic neutron sources from (α,n) reactions in oxide compounds calculated from the R-matric theory,” EPJ manuscript (in preparation, 2019).

APPENDIX A. REFERENCE ^{252}Cf-SOURCE EMISSION RATE CHECK BY ABSOLUTE NEUTRON COINCIDENCE COUNTING AND ASSOCIATED UNCERTAINTY QUANTIFICATION USING THE MINI-ENMC

APPENDIX A. REFERENCE ^{252}CF-SOURCE EMISSION RATE CHECK BY ABSOLUTE NEUTRON COINCIDENCE COUNTING AND ASSOCIATED UNCERTAINTY QUANTIFICATION USING THE MINI-ENMC

Absolute neutron coincidence counting (NCC) was recently realized to have the potential to determine the neutron production rate in ^{252}Cf sources to high accuracy. Such sources are routinely used to both characterize and efficiency calibrate neutron detectors, so this capability is of interest not just to nuclear safeguards but also to the neutron measurement community. In this context, by high accuracy we mean comparable with or better than the present certification provided by national standards laboratories using the long-established absolute $MnSO_4$-bath technique [A-1, A-2]. The ABsolute Californium Determination (ABCD) method using NCC allows some users to independently check the emission rate of a certified source (which is always a good experimental practice) or, in some circumstances, perhaps even self-certify a source at a similar or higher level of accuracy as a national metrology laboratory. The primary reference source used in this work was FTC-CF-1830, and we adopted the emission rate established by the U.S. National Institute of Standards and Technology (NIST) using their $MnSO_4$-bath. But as a check, we undertook the absolute NCC measurement described below. This is an important aspect of the present UF_6(α,n) measurement campaign because it independently confirms the absolute scale of the measurements.

Because of time constraints, run times were kept quite short—typically only 180 sec, or sometimes 300 sec per point. However, compared to prior work which established ABCD, we take advantage of a recent evaluation of ^{252}Cf nu-bar and provide a detailed propagation of variance (POV) and the associated uncertainty budget.

To briefly recap the ABCD method by NCC technique, the point-model equations for a ^{252}Cf source after dead time correction (DTC), background subtraction and extrapolation to zero shift-register pre-delay and infinite coincidence gate width are

$$S_c = F(\varepsilon_f \upsilon_1 + \varepsilon_d \upsilon_d)\,, \tag{A.1}$$

$$D_{c,\infty} = F\varepsilon_f^2 \frac{\upsilon_2}{2}\,, \tag{A.2}$$

where

F is the spontaneous fission rate taking place in the source capsule,

υ_1, also commonly referred to as prompt nu-bar, is the average number of prompt fission neutrons emitted following spontaneous fission,

υ_d is the average number of delayed neutrons emitted following fission,

ε_f is the neutron detection efficiency, counts per neutron, for neutrons produced in the source with a prompt fission neutron energy spectrum (PFNS),

ε_d is the corresponding value for delayed neutrons,

and,

$\upsilon_2{}' = \langle \upsilon(\upsilon - 1) \rangle'$ is the second factorial moment of the prompt fission neutron multiplicity launch distribution.

These equations assume that non-ideal detector behavior, such as double pulsing, is negligible. This can be demonstrated experimentally using a variety of diagnostics and by counting a near random neutron source [A-3]. The method also relies on the ability to extrapolate to infinite gate without unidentified bias.

The neutron emission rate from the ^{252}Cf *inside* the source capsule (the capsule being part of the detector in this description of the physical response) is given by

$$Y = F(\upsilon_1 + \upsilon_d). \tag{A.3}$$

Substituting this definition into the previous expressions for the singles and doubles rates we find, after some rearranging, that

$$S_c = \frac{Y}{\upsilon_1\left(1 + \frac{\upsilon_d}{\upsilon_1}\right)} \varepsilon_f \upsilon_1 \left(1 + \frac{\varepsilon_d \upsilon_d}{\varepsilon_f \upsilon_1}\right), \tag{A.4}$$

$$D_{c,\infty} = \frac{Y}{\upsilon_1\left(1 + \frac{\upsilon_d}{\upsilon_1}\right)} \varepsilon_f^2 \frac{\upsilon_2}{2}. \tag{A.5}$$

From the expression for S_c, the detection efficiency for fission spectrum neutrons may be written as

$$\varepsilon_f = S_c \frac{\left(1+\frac{\upsilon_d}{\upsilon_1}\right)}{Y} \frac{1}{\left(1+\frac{\varepsilon_d \upsilon_d}{\varepsilon_f \upsilon_1}\right)}. \tag{A.6}$$

Using this result in the equation for $D_{c,\infty}$ gives

$$D_{c,\infty} = \frac{Y}{\left(1+\frac{\upsilon_d}{\upsilon_1}\right)} \left(S_c \frac{\left(1+\frac{\upsilon_d}{\upsilon_1}\right)}{Y} \frac{1}{\left(1+\frac{\varepsilon_d \upsilon_d}{\varepsilon_f \upsilon_1}\right)} \right)^2 \frac{1\upsilon_2}{2\upsilon_1}. \tag{A.7}$$

Solving for Y yields

$$Y = \left(\frac{S_c^2}{D_{c,\infty}}\right) \frac{\left(1+\frac{\upsilon_d}{\upsilon_1}\right)}{\left(1+\frac{\varepsilon_d \upsilon_d}{\varepsilon_f \upsilon_1}\right)^2} \frac{1}{2} \upsilon_1 \left(\frac{\upsilon_2}{\upsilon_1^2}\right), \tag{A.8}$$

which leads to the following measurement equation for neutron yield:

$$Y = \left(\frac{S_c^2}{D_{c,\infty}}\right) \cdot \left[\frac{\left(1+\frac{\upsilon_d}{\upsilon_1}\right)}{\left(1+\frac{\varepsilon_d \upsilon_d}{\varepsilon_f \upsilon_1}\right)^2} \right] \cdot \frac{\upsilon_1 \Gamma_2}{2}, \tag{A.9}$$

where we have introduced the second-order Diven's parameter $\Gamma_2 = \frac{\upsilon_2}{\upsilon_1^2}$.

Diven's parameters (they can be defined in a similar way for higher moments) are especially useful pieces of experimental data that can be evaluated and used to represent the statistical properties of the prompt fission neutron multiplicity distribution because they are independent of detector efficiency. This means that data sets from different experimental groups may yield accurate Γ_2 estimates even if their absolute efficiencies are not well established. Hence, in our case we may use an evaluated value of Γ_2 and combine it with a separately estimated value of υ_1 to set the scale of the second factorial moment. This is a novel interpretation of basic nuclear data that has great pragmatic value in the practice of neutron correlation counting for nuclear safeguards.

For the purposes of uncertainty quantification (UQ), we use the nuclear data parameters of pure ^{252}Cf. This is appropriate since the contribution from the ^{250}Cf content present in the source is quite small and can be allowed for with negligible error.

The average number of delayed neutrons emitted following spontaneous fission is based on the experimental studies of Cox et al. [A-4] and Smith et al. [A-5].

$$\upsilon_d = (0.0086 \pm 0.0011)\, n.fis^{-1}. \tag{A.10}$$

The mean number of prompt fission neutrons emitted following fission, υ_1, has recently been reviewed by Croft et al. [A-6]. There are 14 high-quality absolute determinations, and the recommended value involved a careful review of each and allowed for any identified correlations between them. The recommended value is

$$\upsilon_1 = (3.7573 \pm 0.0056), n.fis^{-1}. \tag{A.11}$$

The ratio $\frac{\varepsilon_d}{\varepsilon_f}$ of the detection efficiency for delayed neutrons to the efficiency for fission spectrum neutrons was replaced by the quantity $r = \omega \cdot \frac{\varepsilon_{AmLi}}{\varepsilon_{Cf}}$, where $\varepsilon_{AmLi} = 0.7760\ cnt.n^{-1}$ is the measured efficiency using known AmLi sources determined as part of this work; $\varepsilon_{Cf} = 0.6011\ cnt.n^{-1}$ is the efficiency measured using a known ^{252}Cf source from prior work as reported by Menlove et al. [A-7]; and ω is a scale factor to account for the difference between the delayed neutron spectrum and the AmLi spectrum that we are taking as a close experimental analog [A-8]. The uncertainties in the measured efficiencies are dominated by the uncertainties in the emerging emission rates of the reference sources. For the AmLi sources used, the uncertainty is approximately 3% and the ^{252}Cf source uncertainty is approximately 1%; both are directly traceable to NIST $MnSO_4$-bath measurements (but note that from separate experimental investigations we believe the uncertainty for the AmLi source is generously high by a factor of perhaps three). Lacking strong experimental evidence about the complete delayed neutron spectrum for ^{252}Cf [A-9], we took $\omega = (1.00 \pm 0.05)$. Because of competitive capture between the ^{3}He in the proportional counters and the other materials of the mini-ENMC, and also leakage from the counter, it is not feasible for ε_{AmLi} to be larger than 0.85 cnt·n^{-1}, and because the AmLi spectrum is softer than that of ^{252}Cf, we know that $r > 1$. Thus, our choice of ω uncertainty allows for a generous spread (e.g., at 95% confidence corresponding to two standard deviations).

The current best estimate of Diven's parameter of second order is taken from the review of Croft et al. [Santa Fe 2016].

$$\Gamma_2 = (0.846827 \pm 0.000462)\ , \tag{A.12}$$

where the uncertainty is stated at the 68.3% confidence interval based on nine independent experimental determinations and includes a coverage factor of approximately 1.067 to account for eight degrees of freedom.

The experimental quantity $\left(\frac{S^2}{D}\right)$ extrapolated to zero pre-delay and infinite gate width was determined from a series of measurements performed with FTC-CF-1830 arranged axially at the center of the mini-ENMC measurement cavity. We shall outline how the extrapolated value was estimated. Note, however, when combining count data for a given source from different campaigns, or from within a campaign that extends over several days, we routinely work first in terms of the $\frac{D}{S}$ ratio because, in this form, data taken at different times do not need to be decay corrected since the ratio is self-normalizing (the decay rate is about -0.0072 %/day). In this work we used a JSR-15 Multiplicity Shift-Register (MSR) module [A-10] and INCC ver.5.1.2 software [A-11] to collect the data. Compared with list mode data acquisition, this has the disadvantage that the measurements are time-consuming in the sense that every (T_p,T_g) setting has to be made manually with the operator in attendance (rather than collecting a single long run which can be analyzed off-line). On the other hand, it has the distinct benefit that each counting experiment is statistically independent, which considerably simplifies subsequent (statistical) interpretation of the measurements.

In one campaign, $\frac{D}{S}\ vs\ T_g$ over the interval 3 μs to 512 μs was measured with T_p held fixed at 1.5 μs (the usual operational setting for the mini-ENMC to place the coincidence gate in a region free from dead time and baseline transients on the pulse train). Fitting the data by minimizing chi-squared over the interval from 48 μs to 512 μs (seven points) to a two model-parameter saturating exponential

($C \cdot \left[1 - exp\left(-T_p/\tau_{eff}\right)\right]$) gave an effective dieaway time, τ_{eff}, of approximately 24.5 μs. The quality of the fit was not high (chi-squared per degree of freedom of about 4.3) but was adequate to establish that for T_g-values above or about 250 μs the doubles response is fully saturated for practical applications. A relatively long (179 cycles of 20 sec), high-precision count at $T_g = 250\ \mu s$ was then performed and was used to establish the experimental $\left(\frac{S^2}{D}\right)$-value with a "very long" gate width but finite (standard) pre-delay setting of 1.5 μs. This is an intermediary step toward obtaining a fully extrapolated value. Chance, or accidental, coincidences were subtracted from the number of real (or genuine) plus accidental coincidence obtained from the shift-register logic using the calculated accidentals method: $A_{calc} = S_m \cdot T_g \cdot t, cnts$, where A_{calc} is the number of counts in the cycle, t is the cycle collection time, S_m is the observed (or

measured) singles counting rate, and T_g is the coincidence gate width. For each cycle the rates were dead time and the background was corrected before forming the ratio. Dead time corrections were made using the semiempirical formalism [A-12, A-13] with coincidence dead time parameter $d = A + B.S_m, \mu s$. Values of the coincidence dead time parameters A and B had been previously measured at 0.140 μs and 0.005×10^{-6} μs per cnt/s, respectively [A-7]. The deadtime correction for the singles squared-to-doubles ratio is approximately 0.988, so a 5% uncertainty in the value of the deadtime parameter translates to a factional uncertainty in the correction factor of about 0.062%. A possible systematic uncertainty of 5% on the dead time parameter, d, was propagated into the final result. The correction for doubles background is very small, but for completeness an adjusted background value was used for each gate setting by scaling the 24 μs value for the gate utilization factor. The resulting mean value of $\left(\frac{S^2}{D}\right)_{T_p = 1.5, T_g = 250}$ obtained was (175690 ± 152) cnt/sec where the uncertainty is the standard error. The individual rates varied from 170915 to 181762 cnt/sec with 68.3% of observations lying roughly in the interval, 173590 to 177730 cnt/sec, which compares favorably with the mean plus/minus the sample standard deviation range of 173661 to 177719 cnt/sec. The data is reasonably well represented by a normal distribution using the sample mean and sample deviation.

In another series of measurements, $\frac{D}{S} vs\ T_p$ over the interval 0.25 μs to 4.00 μs was measured with T_g held fixed at 24 μs (the usual operational setting). A supplementary set of data with T_g held fixed at 3 μs was also collected. Below 1 μs the $T_g = 3\ \mu s$ showed some roll off due to dead time and baseline recovery effects, but above 1 μs the shape of the doubles dieaway was consistent with the $T_g = 24$ μs data. An exponential fit ($a \cdot e^{-b \cdot T_p}$) to the 24 μs data returned a measured value of $b = \frac{1}{\tau_S}$, the reciprocal effective dieaway time, in this short pre-delay region of 0.055664 μs^{-1} (corresponding to $\tau_S \approx 18\ \mu s$). The relative standard uncertainty on b is estimated to be 0.122% from the standard error obtained from the fit scaled by a coverage factor of 1.067 to account for 8 degrees of freedom. Using this b value, the factor by which the doubles rate is less when using a finite pre-delay (of 1.5 μs) is calculated as

$P = \exp(-b \cdot T_p)$. This is a relative correction applied to the selected large gate value $\left(\frac{S^2}{D}\right)_{T_p = 1.5, T_g = 250}$. It does not depend on when it was determined. In the procedure described here, the date and time of the source strength determination is solely set by the time that $\left(\frac{S^2}{D}\right)_{T_p = 1.5, T_g = 250}$ was measured. In our case this was 1pm March 7, 2018 (mid acquisition).

Combining results and being explicit as to how the quantity of interest is calculated we have

$$X = \left(\frac{S_c^2}{D_{c,\infty}}\right) = \delta \cdot P(T_p = 1.5) \cdot \left(\frac{S^2}{D}\right)_{T_p = 1.5, T_g = 250}. \quad \text{(A.13)}$$

Note that although the DTC is made cycle by cycle, the variation is not large because the counting rate for each individual cycle is statistically equal across the data set, so as a mathematical device to propagate the systematic uncertainty in the DTC, we have introduced the factor δ, set numerically equal to unity, but with an associated systematic uncertainty which is propagated into the final result.

Uncertainty Analysis

$$r = \omega \cdot \frac{\varepsilon_{AmLi}}{\varepsilon_{Cf}}. \quad \text{(A.14)}$$

By propagation of variance (POV),

$$\frac{\sigma_r}{r} = \sqrt{\left(\frac{\sigma_\omega}{\omega}\right)^2 + \left(\frac{\sigma_{\varepsilon_{AmLi}}}{\varepsilon_{AmLi}}\right)^2 + \left(\frac{\sigma_{\varepsilon_{Cf}}}{\varepsilon_{Cf}}\right)^2}, \quad \text{(A.15)}$$

$$X = \delta \cdot P \cdot \left(\frac{S^2}{D}\right)_{T_p = 1.5, T_g = 250}, \quad \text{(A.16)}$$

where we have introduced the shorthand $\Lambda = \left(\frac{S^2}{D}\right)_{T_p = 1.5, T_g = 250}$, the selected average value of this quantity. Then

$$\frac{\sigma_X}{X} = \sqrt{\left(\frac{\sigma_\delta}{\delta}\right)^2 + \left(\frac{\sigma_P}{P}\right)^2 + \left(\frac{\sigma_\Lambda}{\varepsilon_\Lambda}\right)^2}, \quad \text{(A.17)}$$

with

$$P = e^{-b \cdot T_p}, \quad \text{(A.18)}$$

$$\frac{\sigma_P}{P} = |-T_p| \cdot \sigma_b, \quad \text{(A.19)}$$

where $T_p = 1.5\ \mu s$ in our case.

Writing the measurement equation as

$$Y = X \cdot \left[\frac{\left(1 + \frac{\upsilon_d}{\upsilon_1}\right)}{\left(1 + r \cdot \frac{\upsilon_d}{\upsilon_1}\right)^2} \right] \cdot \frac{\upsilon_1 \cdot \Gamma_2}{2}, \tag{A.20}$$

the fractional uncertainty contribution $\left(\frac{dY}{Y}\right) = \left|\alpha \cdot \frac{\partial Y}{\partial \alpha} \cdot \left(\frac{\sigma_\alpha}{\alpha}\right)\right|$ for each of the five principal independent variables is summarized in the table. Note that in deriving the analytical expressions listed for the variables υ_d and υ_1, it is useful to first show that given the function $h(x) = \frac{T(x)}{L^2(x)}$, the derivative h' of $h(x)$ with respect to x is $h' = \left(\frac{T'}{T} - 2\frac{L'}{L}\right)$.

Parameter	$\left(\frac{dY}{Y}\right)$	Value %
X	$\left(\frac{\sigma_X}{X}\right)$	0.159
r	$\left\lvert \frac{-2 \cdot r \cdot \frac{\upsilon_d}{\upsilon_1}}{1 + r \cdot \frac{\upsilon_d}{\upsilon_1}} \right\rvert \cdot \left(\frac{\sigma_r}{r}\right)$	0.035
υ_d	$\left\lvert \frac{\frac{\upsilon_d}{\upsilon_1}}{\left(1 + \frac{\upsilon_d}{\upsilon_1}\right)} - 2\frac{r\frac{\upsilon_d}{\upsilon_1}}{\left(1 + r\frac{\upsilon_d}{\upsilon_1}\right)} \right\rvert \cdot \left(\frac{\sigma_{\upsilon_d}}{\upsilon_d}\right)$	0.046
υ_1	$\left\lvert \left(\frac{3 + 2 \cdot \frac{\upsilon_d}{\upsilon_1}}{1 + \frac{\upsilon_d}{\upsilon_1}}\right) - \left(\frac{2}{1 + r \cdot \frac{\upsilon_d}{\upsilon_1}}\right) \right\rvert \cdot \left(\frac{\sigma_{\upsilon_1}}{\upsilon_1}\right)$	0.150
Γ_2	$\left(\frac{\sigma_{\Gamma_2}}{\Gamma_2}\right)$	0.055
Combined	Quadrature sum of all five independent contributions	0.232

The fractional total measurement uncertainty is the quadrature sum of the five partial fractional contributions. From the table, this is approximately 0.23%.

For our final yield estimation, we make an additional very small adjustment to allow for the ^{250}Cf contribution to the neutron production. We do this by decay correcting the isotopic composition of the batch of californium used to make the source to the date of present yield determination. For a young

source fabricated from a recently produced batch of californium, the ^{250}Cf contribution should be negligible. For these measurements we estimate that approximately 1.82% of the fissions taking place in the source are attributable to ^{250}Cf. On this basis we estimate that on a per-fission basis, $\upsilon_d = 0.0085$; $\upsilon_1 = 3.7528$; and $\Gamma_2 = 0.846777$. The effect of making these fine adjustments on the resulting yield estimate is however very small. Compared with using pure ^{252}Cf nuclear data, the yield increases by a factor of 1.000040, which is unity within the overall uncertainty budget.

The final experimental neutron production rate is $Y = 256197$ n.s^{-1} with a fractional standard uncertainty of about 0.23%.

For comparison the decay-corrected emission rate of FTC-CF-1830 on March 7, 2018 (also allowing for the small ^{250}Cf contribution based on the source composition provided by the manufacturer) is 253451 n·s^{-1} with a fractional standard uncertainty of approximately 1.05% [A-14].

The two values are within one joint standard deviation of each other, so we conclude that the adopted source emission rate based on the decay-corrected NIST certificate has been successfully independently verified.

Discussion

The limited objective of the present Cf-yield determination measurements was to provide an independent check on the certificate provided by NIST for FTC-CF-1830, since this source was used to set the absolute scale of our UF_6(α,n)–specific yield determination. We consider checking the purity and yield of reference sources to be a good experimental practice in order to avoid unidentified error. Within the combined overall uncertainties stated, our assessment agrees with the decay-corrected calculation, so we have full confidence in the certificate value, which we have therefore adopted in the analysis of our UF_6(α,n) data. Several suggestions for improvements to the method of source strength measurement by the ABCD method using NCC described here can be offered because, according to the uncertainty analysis presented, the method is potentially capable of high accuracy, and our goal was not to approach the ultimate accuracy limit. To do so, it is necessary to pay particular attention to all experimental steps and analysis details. The benefit of highly developing the ABCD technique for ^{252}Cf sources would be the resulting boost it would provide to the entire applied neutron metrology community. Standardized high-density polyethylene moderated arrays for use by standards laboratories would be complementary to the established $MnSO_4$-bath technique but are in many ways easier to set up, maintain, and operate. Furthermore, it would be especially suitable for the weaker sources that challenge the detection limit of the $MnSO_4$-bath. NCCs are extremely stable and well suited to also make relative comparisons of all

types of sources (not just ^{252}Cf). We also extend the analysis to show how the detection efficiency can also be estimated absolutely and directly using a small, sealed, radionuclide ^{252}Cf source.

Before discussing improvements, it is worth reviewing the nature of the ABCD-NCC method. We can rewrite the expression for the yield as follows:

$$Y = \frac{1}{\left(\frac{2 \cdot D_{c,\infty}/S_c^2}{\Gamma_2}\right)} \cdot \left[\frac{\left(1+\frac{\upsilon_d}{\upsilon_1}\right)}{\left(1+\frac{\varepsilon_d \upsilon_d}{\varepsilon_f \upsilon_1}\right)^2}\right] \cdot \upsilon_1. \tag{A.21}$$

Working right to left, the factor υ_1 provides the absolute scaling, and knowing nu-bar absolutely and accurately is key to the potential of the technique; the factor $\left[\frac{\left(1+\frac{\upsilon_d}{\upsilon_1}\right)}{\left(1+\frac{\varepsilon_d \upsilon_d}{\varepsilon_f \upsilon_1}\right)^2}\right]$ corrects for the energy dependence of the NCC and for the delayed neutron contribution given that the measured doubles, υ_1 and Γ_2 pertain only to the prompt fission neutron component—good instrument design and knowledge of the average number of delayed neutrons per fission are emphasized by this term; the measured quantity $\left(\frac{2 \cdot D_{c,\infty}/S_c^2}{\Gamma_2}\right)$ is now clearly seen as having the character of a relative Diven-parameter determination. In basic nuclear physics measurements, Γ_2 can be determined more accurately than nu-bar since it does not depend on detector efficiency. It is usually measured using fission-triggered coincidence counting at low rates to avoid fission neutron burst overlap and requires a specialized fission chamber, and historically most commonly a large liquid scintillation tank. Great care is needed to characterize the capture time distribution, correct for dead time, correct for chance burst overlap, correct for background, ensure that gamma detection is under control, etc. But several high-quality data sets exist for evaluation. In contrast we are using neutron-triggered shift-register coincidence counting logic, a simple sealed radionuclide source of the type that is readily available commercially and in routine use in neutron laboratories, and a standard safeguards neutron detector. The main challenges in determining the quantity $D_{c,\infty}/S_c^2$ have been discussed in the text. Most notably these include dead time correction and extrapolation to zero pre-delay and infinite gate width. We recognize that the factorial doubles rate $D_{c,\infty}$ may also be extracted using different neutron-triggered and random-triggered (that is random with respect to the pulse train) gating schemes and that within each general scheme, nuances exist for how chance coincidences are estimated [A-15, A-16]. But these methods, for example, the Feynman variance-to-mean approach [A-17], are all

based on the same physical interpretation of the detector response and pulse train and ought to give the same expectation value.

We now itemize areas for refinement; this is done to approach the ultimate limit of the method.

The calculated correction for dead time is an important source of potential systematic error, and its fractional importance increases with source strength. The dead time model is not perfect, so it is beneficial to keep the rate losses low. By using additional preamplifier/discriminator (P/A) boards and optimizing the ^{3}He proportional counter–P/A combination, a reduction in rate losses by a factor of three or more can be readily achieved. Different DTC models and techniques are also available [A-18; A-19, A-20, A-21], and a sensitivity study between them should be performed. Comparison to first-principles analog simulations (from ionization track to registration) is also recommended.

We have not corrected for any neutron losses/gains due to neutron interactions in the type 304 stainless steel source encapsulation. For the Model 10S capsule (O.D 5.5 mm, H 11.9 mm, welded top plug 3.9 mm, base 1.8 mm, side wall 0.8 mm), the losses are expected to be small. A Monte Carlo calculation would quantify this statement. Experimental confirmation of the wall effect is possible [A-22].

We elected to perform a 1 hr count with $T_g = 250\ \mu s$ to determine the best single value for an infinite gate width setting. In future work we suggest using $T_g = 512$ μs and counting longer (in part to compensate for the higher accidentals) as an extra precaution. However, if time constraints are more forgiving than was the case here, it would be good practice to perform long counts at several values of large gate width to directly ensure the doubles rate is fully saturated. Theoretically there could be a weak long-lived time component due to escaped neutrons scattering back into the counter from the floor and other materials nearby. Our doubles estimate could therefore be slightly underestimated (on the order of 0.1%, say), which means the yield could be slightly over-reported as a result. Care in placing the detector and neutronically isolating it from its surroundings should be examined in this context.

In our work the D/S data used to extrapolate to zero pre-delay were collected separately from the data used to establish the long gate width behavior. A preferred practice would be not to reposition the source during its characterization. However, we are confident on physical grounds that the extrapolation factor, $P = e^{-b \cdot T_g}$, from zero pre-delay to finite pre-delay, is insensitive to source positioning (which is better than 1 mm) since we are only interested in extracting the effective reciprocal dieaway parameter, which is governed by the moderate detector assembly. However, in this work to estimate the value of b, the reciprocal effective dieaway time, we used a fit over the interval $T_p = 0.25$ μs to 4.00 μs with $T_g = 24$ μs

. Again, only short (typically 180 sec) runs were made at each point and longer runs are warranted to improve overall precision. However, we must also consider the possibility that at short pre-delay values the D/S curve will roll over due to dead time and baseline transients. Excluding the points at 0.25 μs and 0.50 μs and fitting only over the interval $T_p = 1.00$ μs to 4.00 μs altered the value of P from 0.9199 to 0.9188, a reduction by a factor of 0.999 which would also apply to the yield; this would signal that our reported value could be too high by about 0.1 %. The standard relative uncertainty on the P-value also increased from approximately 0.12 % to 0.17 %, in part because of the fewer degrees of freedom and the longer projected distance measured from the centroid of the experimental data. Hence, within our stated errors, our result stands. Although we did rudimentary tests to show that the effective dieaway in this short pre-delay regime is the same within experimental error when a gate width of 3 μs is used instead of 24 μs, a more detailed scrutiny of the assumption that the estimated P-factor applies to *all* coincidence gate settings (including and especially the selected value of T_g=250 μs) should be undertaken. Because the mini-ENMC exhibits almost single exponential behavior (by virtue of the Cd-liner and high population density of high-pressure ^{3}He proportional counters in the polyethylene moderator), we expect it to be a reasonable approximation. Some additional reassurance is provided by the fact that the two estimates for dieaway, which emphasize the very short-term and very late-term neutron dynamics in the counter, are fairly close in value ($1/b = 18\ \mu s$ vs $\sim 24.5\ \mu s$ from the wide gate width data).

Another basic physics question is whether the dieaway time is well approximated by an exponential form at very short pre-delay values. To appreciate this comment, consider a fission burst of fast neutrons striking the counter. The neutrons in the burst are not detected with high efficiency until they have been slowed by the moderator. The doubles rate is an event-triggered tally, and so the observed doubles die-away time is a convolution of the detection time distribution (reference to the time of fission), which will start low and peak before decaying. The convolution is therefore not exponential until after some short (pre-delay) time. The ideal (with a perfect detector system) doubles die-away time structure can be studied using Monte Carlo transport simulation and the magnitude of such an effect quantified.

The doubles dieaway time can be reduced somewhat and any vestigial long-lived harmonic further suppressed by more effectively poisoning the moderator. One way to do this is to use more, but smaller diameter, high-pressure ^{3}He proportional counters so that slow neutrons have less distance to travel to an absorption site. Of course, the cavity diameter is quite large, being intended to accept storage cans of PuO_2 and MOX powders, meaning that another ring of detectors can be added using an insert.

The energy dependence can also be flattened to some degree by the arrangement of proportional counters in the annular moderator. The use of a smaller cavity and neutron detectors in the end-plugs can also

increase the efficiency. The benefit of an ultrahigh efficiency is that the fractional difference between the efficiency for neutrons emitted with a delayed neutron spectrum and with a fission spectrum is less and the range of potential variation is also narrowed. Therefore, the $\varepsilon_d/\varepsilon_f$ can be estimated with greater confidence.

Our choice of Γ_2-value is based on the mean of nine experimental estimates. A refinement would be to review each measurement to estimate the quality of each determination so that a weighted estimate can be made instead.

Fission-triggered methods commonly used to measure the prompt fission multiplicity distribution are insensitive to delayed neutron processes that result in the emission of two or more neutrons. In contrast, the neutron-triggered multiplicity counting technique we are using to determine the ^{252}Cf-source emission rate responds to such delayed-neutron processes as if they are fission bursts. In the present analysis we have not considered the impact of this potential physical process, although it can be anticipated to be small—a fraction of a percent of the already small relative delayed neutron fraction.

Determining the Detection Efficiency

Until Appendix A, we have focused on using absolute NCC to experimentally determine the total emission rate, Y, of a physically small, sealed, radionuclide neutron source of ^{252}Cf. Because the $MnSO_4$-bath determines the total emission rate, the measured and certificate values can be compared. Our principal point-model equations may instead be solved to determine the fission neutron and average neutron detection efficiencies.

$$S_c = F(\varepsilon_f \upsilon_1 + \varepsilon_d \upsilon_d)\,. \tag{A.22}$$

$$D_{c,\infty} = F\varepsilon_f^2 \frac{\upsilon_2}{2}\,. \tag{A.23}$$

$$Y = F(\upsilon_1 + \upsilon_d)\,. \tag{A.24}$$

Rearranging gives the measurement equation for prompt fission spectrum neutrons:

$$\varepsilon_f = \left(\frac{\frac{D_{c,\infty}}{S_c}}{\frac{\upsilon_1 \cdot \Gamma_2}{2}}\right) \cdot \left(1 + r \cdot \frac{\upsilon_d}{\upsilon_1}\right), \tag{A.25}$$

where we are assuming that the efficiency ratio $r = \frac{\varepsilon_d}{\varepsilon_f}$ can be estimated independently, for instance via a Monte Carlo neutron transport calculation based on knowledge of the two spectra and of the detector design. The factor $\left(1 + r \cdot \frac{\upsilon_d}{\upsilon_1}\right)$ is close to unity in all practical cases but cannot be ignored if results accurate to a few tenths of a percent are needed. Taking care to estimate r is therefore important, although the uncertainty in υ_d is currently substantial (about 13%), so the uncertainty in $r \cdot \frac{\upsilon_d}{\upsilon_1}$ is inherently limited by nuclear data. A new and accurate measurement of the delayed neutron yield of ^{252}Cf is long overdue considering ^{252}Cf is a de facto reference standard in fission studies.

The average efficiency to Cf-source neutrons is defined by the way it is measured using a known source:

$$\varepsilon_{Cf} = \frac{S_c}{Y} = \left(\frac{\frac{D_{c,\infty}}{S_c}}{\frac{\upsilon_1 \cdot \Gamma_2}{2}}\right) \cdot \frac{\left(1 + r \cdot \frac{\upsilon_d}{\upsilon_1}\right)^2}{\left(1 + \frac{\upsilon_d}{\upsilon_1}\right)}, \tag{A.26}$$

where the right-hand side of the expression is obtained by substituting our previously obtained expression for Y.

The relationship between ε_f and ε_{Cf} is seen by inspection to be

$$\varepsilon_{Cf} = \varepsilon_f \cdot \frac{\left(1 + r \cdot \frac{\upsilon_d}{\upsilon_1}\right)}{\left(1 + \frac{\upsilon_d}{\upsilon_1}\right)}, \tag{A.27}$$

which can also be seen immediately by equating the two expressions for the single rate per fission, $\frac{S_c}{F}$:

$$\varepsilon_{Cf} \cdot (\upsilon_1 + \upsilon_d) = (\varepsilon_f \upsilon_1 + \varepsilon_d \upsilon_d). \tag{A.28}$$

Having established the detection efficiency for the ^{252}Cf PFNS, the efficiency for other fissioning systems can be estimated by multiplying it by a calculated relative efficiency factor. The doubles rate for another fissioning system can be scaled using nuclear data parameters. The doubles rates for a finite gating structure can be scaled by using an experimentally estimated doubles gate utilization factor $f_d = \frac{D_c(T_p, T_g)}{D_c(0,\infty)}$. This is the one way in which ^{252}Cf can be used to calibrate a NCC for the assay of ^{240}Pu$_{\text{eff}}$-mass. However, the uncertainty introduced by these additional steps means that the overall uncertainty is

currently much poorer that can be obtained using known Pu items to perform a direct mass calibration. What is needed for applied safeguards work is a direct experimental determination of the $^{240}Pu_{eff}$ gram equivalent of ^{252}Cf per fission (rather than the current way basic nuclear data is evaluated). This may be achieved by comparing suitable Pu reference items to ^{252}Cf sources using the methods discussed. The technique of characterizing ^{252}Cf very accurately, as discussed here, then becomes far more powerful for calibrating passive neutron correlation counters.

In the present work we measure the neutron detection efficiency for ^{252}Cf neutrons and estimate the efficiency for $UF_6(\alpha,n)$ neutrons by multiplying the result by an item-specific calculated efficiency ratio based on adopted spectra. By using a spread of plausible spectra, the derived efficiency is bounded. By calculating the efficiency ratio, bias associated with the physics fidelity of performing the neutron transport is considerably reduced compared to making an absolute calculation. The end result is therefore grounded (or benchmarked) to the experiment

REFERENCES FOR APPENDIX A

[A-1] S. Croft and D. Henzlova, "Determining ^{252}Cf source strength by absolute passive neutron correlation counting," *Nucl. Instrum. Meths. Phys Res*. A714 (2013) 5-12.

[A-2] D. Henzlova, A. Favalli, and S. Croft, "In-Depth Evaluation of ^{252}Cf Absolute Calibration by Passive Neutron Correlation Counting Method. Metrologia," accepted for publication.

[A-3] A. S. Moore, S. Croft, R. D. McElroy Jr., and J. P. Hayward, "Methods for Diagnosing and Quantifying Double Pulsing in a Uranium Neutron Collar System Using Shift Register Logic," *Nucl. Instrum. Meths. Phys Res. A*, submitted (2019).

[A-4] S. Cox, P. Fields, A. Friedman, R. Sjoblom, and A. Smith, "Delayed neutrons from the spontaneous fission of ^{252}Cf," *Phys. Rev.* 112(3) (1958) 960-963.

[A-5] A. Smith, P. Fields, A. Friedman, S.A. Cox, and R. Sjoblom, An experimental study of fission in the actinide elements, Proc. 2nd International Conference on the Peaceful Uses of Atomic Energy, United Nations, NY. A/CONF.15/P/690(June 1958) 12pp.

[A-6] S. Croft, A. Favalli, and R.D. McElroy Jr., "A review of the prompt neutron nu-bar value for ^{252}Cf spontaneous fission," *Nucl. Instrum. Meths. Phys Res. A*, in press.

[A-7] H.O. Menlove, M.T. Swinhoe, J.B. Marlow, D.G. Langner, M.R. Newell, and C.D. Rael, *Mini-Epithermal Neutron Multiplicity Counter (miniENMC) Manual*, Los Alamos National Laboratory manual report LA-14350-M (November 2007).

[A-8] J.G. Owen, D.R. Weaver, and J. Walker, "Neutron spectra from Am/F and Am/Li (α,n) sources," International Conference on Nuclear Data for Science and Technology, Antwerp, 6-10 September 1982, pp 492-495.

[A-9] E.T. Chulick, P.L. Reeder, C.E. Bemis, and E. Eichler, "Energy spectrum of delayed neutrons from the spontaneous fission of ^{252}Cf," *Nuclear Physics A* 168 (1971) 250-258.

[A-10] N. Menaa, M. Villani, S. Croft, B. McElroy, R. Venkataraman, S. Philips, and M. Newell, Evaluation of the LANL handheld multiplicity shift register and Canberra JSR-15 NSS/MIC IEEE, October 28-November 3, 2007 Conference Proceedings, Honolulu, Hawaii,

[A-11] Bill Harker and Merlyn Krick with Joe Longo, *INCC Software Users Manual*, Los Alamos National Laboratory, Safeguards Science and Technology Group (N-1), Nuclear Nonproliferation Division (November 1, 2005).

[A-12] H.O. Menlove and J.E. Swansen, "A high-performance neutron time correlation counter," *Nuclear Technology* 71(No., 1985) 497-505.

[A-13] J.E. Swansen, "Deadtime reduction in thermal neutron coincidence counter," *Nucl. Instrum. Meths Phys. Res. B* 9 (1985) 80-88.

[A-14] National Institute of Standards and Technology (NIST), *Report of Calibration, Neutron Source Strength Calibration Report Test Number 285873 for Source FTC-CF-1830 on reference data,* September 17, 2014.

[A-15] S. Croft, D. Henzlova, and D.K. Hauck, "Extraction of correlated count rates using various gate generation techniques: Part I Theory," *Nucl. Instrum. Meths Phys. Res. A* 691 (2012) 152-158.

[A-16] D. Henzlova, S. Croft, H.O. Menlove, and M.T. Swinhoe, "Extraction of correlated count rates using various gate generation techniques: Part II Experiment," *Nucl. Instrum. Meths Phys. Res. A* 691 (2012)159-167.

[A-17] S. Croft, A. Favalli, D.K. Hauck, D. Henzlova, and P.A. Santi, "Feynman variance-to-mean in the context of passive neutron coincidence counting," *Nucl. Instrum. Meths Phys. Res.* A686 (2012) 136-144.

[A-18] L. Holzleitner and M.T. Swinhoe, "Dead-time correction for any multiplicity using list mode neutron multiplicity counters: A new approach – Low and medium count-rates," *Radiat. Meas.* 46 (2011) 340-356.

[A-19] S. Croft, L.G. Evans, A. Favalli, D.K. Hauck, D. Henzlova, and P. Santi, "Revisiting the form of dead time corrections for neutron coincidence counting," Radiat. Meas. 47 (2012) 467-474.

[A-20] D.K. Hauck, S. Croft, L.G. Evans, A. Favalli, P.A. Santi, and J. Dowell, "Study of a theoretical model for the measured gate moments resulting from correlated detection events and an extending dead time," *Nucl. Instrum. Meths. Phys. Res*. A719 (2013) 57-69.

[A-21] S. Croft and A. Favalli, "Extension of the Dytlewski-style dead time correction formalism for neutron multiplicity counting to any order," *Nucl. Instrum. Meths Phys. Res*. A869 (2017) 141-152.

[A-22] R. Weinmann-Smith, S. Croft, M.T. Swinhoe, and A. Enqvist, Changes to the ^{252}Cf neutron spectrum caused by source encapsulation, ESARDA Bulletin, Issue 54 June 2017 pp44-53. ISSN 0392-3029.

APPENDIX B. RADIOLYSIS

APPENDIX B. RADIOLYSIS

Considerable information on the properties of UF_6, particularly about its safe handling, conversion, enrichment, and fuel fabrication, can be found in [B-1]]. Long-term stability is of concern since, as we are reminded by NRC [B-2], UF_6 is dynamic substance even when thermal processes can be ignored because chemical reactions can be induced by ionizing radiation via the process known as radiolysis. Consequently, one can expect a slow and spontaneous dissociation or decomposition of highly enriched UF_6 due to the self-irradiation by ^{234}U α-particles [B-3]. It is well known that for the actinides, energy deposition is dominated by α-tracks [B-4]. It has also been suggested that α-particles in bulk UF_6 are considerably more effective for a given amount of energy deposited at breaking chemical bonds [B-2] than other forms of ionizing radiation (e.g. x-, γ- and β-rays). Trowbridge et al. [B-5] in Table 2 on page p. 19 of [B-5], which refers to Saraceno on page 26 of [B-6], summarize fluoride radiolysis of uranium fluorides and Molten Salt Reactor Experiment (MSRE) salts. They give the radiation chemical yield, *G,* value of 1.5 molecules of fluorine, F_2, produced per 100 eV of absorbed radiation for α-radiation in solid UF_6. The corresponding value quoted for x- and γ-radiation (which liberate fast electrons that cause most of the associated ionization) is considerably lower at only 0.02. Both values likely have large uncertainties given the sparse semi-theoretical and experimental data on which they are based and the difficulties associated in performing the experiments on uranium, which has a low specific activity and hence low rate of gas production (and, in these studies, pressure due to gas production was being used as the direct observable, rather than say optical spectroscopy [B-7]). Being one of the few published reports on radiolysis in UF_6, Saraceno [B-6] has been widely adopted. Our narrow interest is to quantify whether the rate of radiolysis is high enough to affect the (α,n) production rate for the range of items (enrichment and age) we measured. Our problem is that we do not know how to rigorously assess the accuracy of the G values presented by Saraceno [B-6] and therefore any conclusions made by assuming Sareceno's recommended value.

The G value proposed by Saraceno [B-6] is actually an upper bound, assuming no reverse (reformation or back reaction or long-term dynamic-equilibrium that might be established in a sealed system) and that every ion pair formed results in decomposition of one UF_6 molecule. The number of ion pairs per α-particle assumed by Saraceno was 0.137×10^6 i.p./^{234}U α-particle taken from Bernhardt et al. [B-8] for UF_6 gas based on ionization data measured by Steidlitz et al. [B-9]. Steidlitz et al. studied 13 gases, including a range of fluorocarbon gases, for which the average energy, *w*, needed to create an ion pair was within about 10% 30 eV/i.p. in all cases. They also confirmed additivity scaling rules for both range and ionization. We shall return to this discussion later.

Bernhardt et al. studied UF_6 radiolysis using radon (^{222}Rn) as the α-source. The chemical reaction may be represented as follows:

$$UF_6 \overset{\alpha}{\rightleftarrows} UF_x + \left(\frac{6-x}{2}\right) \cdot F_2. \tag{B.1}$$

The solid product was designated as UF_x because it could be eiher UF_4 or UF_5 but could not be identified because of the small amounts generated. For our purposes, we are primarily concerned with the loss of F(α,n)-targets in the medium, so if we assume $x = 5$, consistent with the characterization of solid uranium fluorides in UF_6-storage cylinder heels, and ignore the back reaction, on this basis we have

$$2 \cdot UF_6 \xrightarrow{\alpha} 2 \cdot UF_5 + F_2, \tag{B.2}$$

and G is the number of molecules of F_2 produced per 100 eV of radiation energy deposited. Across a series of nine experiments (with no additional diluent gases present) Bernhardt et al. obtained G values ranging from about 0.24 to 0.70, the mean values being (0.45±0.05), where the uncertainty is the statistical standard error only. In a second series of measurements with nitrogen added, a wide range of results was again obtained with extracted G values extending to approximately 2.8. In addition to the random scatter, Bernhardt et al. caution that systematic bias, such as other unidentified dissociation mechanisms, which are difficult to quantify, may also be present in one of both types of experiment.

Dmitrievskii et al. [B-10] was primarily concerned with the decomposition of UF_6 under fission fragment irradiation. From both new experimental data and a search of the available literature, a G value of about 0.4±0.05 was obtained for fission fragments, again with a potentially large additional systematic uncertainty. They also found UF_6 dissociation by fast electrons to be negligible in comparison (with a G on the order of 0.005 stated in the text, although the value is 0.06 if we use the alternative statement of 0.045 moles of UF_6 per kWh).

Trowbridge et al. [B-5] reviewed experimental radiolysis data reported in the literature with an emphasis on experimental molten salt reactor fuel. Some unconvincing arguments are made to justify that G-values for x-, γ-, and fast electron radiation is much less than that for α-radiation (although this does not matter for purposes of our discussion because α-radiation dominates the energy deposition). The relevant experimental data considered is mainly from the K-25 group at the Oak Ridge Gaseous Diffusion Plant reported prior to the report by Bernhardt et al. Again, they find a large variation in G-values, roughly spanning the range from 0.085 to 0.43, with a mean of about 0.5 molecules of F_2 per 100 eV in the case of

UF_6 gas subject to ^{220}Rn. The estimated value of Saraceno [B-6], 1.5 molecules of F_2 per 100 eV, discussed earlier, is also included in Bernhardt's review.

Given the scant experimental data and concerns over both the precision and accuracy of the direct experimental data, one can appreciate why Saraceno's estimate is included as a legitimate, technically defensible, and conservative choice. However, the overall situation is clearly unacceptable from a scientific perspective since in principle it is feasible to determine the quantity with far better precision and accuracy than is exhibited in the current literature.

Adopting Saraceno's logic then, if 0.137×10^6 ion pairs are formed per ^{234}U α-particle and each ionization results in one molecule of UF_6 being dissociated into $UF_5+\frac{1}{2}F_2$ and given the mean α-particle energy emitted by ^{234}U is 4.75926×10^6 eV [B-11], we find $4.75926/0.137=34.74$ eV is needed on average per UF_6 dissociation or 69.48 eV per molecule of F_2 produced. The G-value is therefore $100/69.48=1.44$ (rounded to 1.5) molecules of F_2 per 100 eV. The assumption that every $(UF_6^+ + e^-)$ ion pair results in a dissociation of a UF_6 molecule means that this estimate is an upper limit for G. Collectively the experimental data supports a lower value. We suggest that a G-value of 0.5 molecules of F_2 per 100 eV is more reasonable (than 1.5) with a relative uncertainty (68% confidence interval) of not less than 20%. Recall too that, for our purposes, fluorine that remains trapped in the (solid) UF_6 matrix and does not emerge into the head space, remains as a potential α-particle target, and is therefore not fully "lost."

In terms of UF_5 (rather than F_2) production, our choice of G value (0.5) equates to one molecule of UF_5 produced per 100 eV of α-energy deposited. For our purposes we assume that the effect of radiolysis is to reduce the (α,n) production rate because instead of stopping in pure UF_6, emergent α-particles are stopped in a mixture of UF_6 and UF_5. Let f be the fraction of UF_6 molecules dissociated into UF_5. Then for $f \ll 1$ we can neglect the dissociation of UF_5, and assuming all the F_2 gas escapes, the (α, n) yield of an aged item can be approximated as

$$Y \approx (1-f)\cdot Y_{UF_6} + f\cdot Y_{UF_5}. \tag{B.3}$$

The estimation of f proceeds as follows. It is well known from the field of nuclear calorimetry [B-4] that for actinide materials which decay by α-emission, for instance the U and Pu isotopes and ^{241}Am, the majority of energy deposited in the material is due to the kinetic energy of the α-particles, with recoil of the daughter nucleus being a small fraction. The range is short, so α-particles are likely to stop within the material, and the escape of γ- and internal conversion electron energy is minor. Spontaneous fission is usually negligible because the low branching ratio more than off-sets the relatively high (about 200 MeV)

energy release per event. With this in mind, for the present purposes of F(α,n) sensitivity analysis, the total radiation deposited per decay may be taken to a high degree of approximation to be equal to the Q-value of the reaction without the need to consider the fine details of the decay scheme; that is, we do not need to treat non α-particle radiation differently.

Because the strongest effect is expected for HEU, we shall assume that the ^{234}U α-emission rate utterly dominates. We know for ^{234}U that the specific α-activity is 2.302×10^{8} Bq/g with a mean α-particle energy of 4.7594×10^{6} eV [B-11]. In one year (365.25 d) 1 g of ^{234}U will therefore dissociate (assuming constant rate):

$$2.302x10^{8}x4.7594x10^{6}x(365.25x24x3600)x\left(\frac{1}{100}\right)\sim3.458x10^{20}\text{ molecules of UF}_6\,.$$

Suppose we start out with a HEU sample of pure UF_6 with a nominal isotopic composition or 1.2, 93.0, and 5.8 wt% in ^{234}U, ^{235}U and ^{238}U, respectively, so that the U molar mass is 237.8254 g. 1 g of ^{234}U corresponds to 1/0.012=83.33 g of U and (83.33/237.8254) × 6.022141×10^{23} = 2.110×10^{23}moles of U. There is one U atom per UF_6 molecule, so the fraction of UF_6 molecules dissociated is

$$f\sim\frac{3.458x10^{20}}{2.110x10^{23}}\sim0.00164. \tag{B.4}$$

To first order (which is all that is justified given our knowledge of the radiation chemical yield, *G,* value) we can scale from this estimate for other isotopic compositions and sample ages. We have purposefully chosen to illustrate the calculation with an extreme (most radiolytically active) example. For recycled material, ^{232}U also needs to be considered. Even at the ppb level, ^{232}U can contribute significantly because of its high specific activity (short half-life) and because it has roughly half a dozen α-particles in its decay chain. The calculation of the fraction *f* requires a more careful temporal treatment to account for the decay chain kinetics.

From our earlier result,

$$\frac{Y}{Y_{UF_6}}\approx(1-f)+f\cdot\frac{Y_{UF_5}}{Y_{UF_6}}, \tag{B.5}$$

and inserting $f\sim0.00164$ for our illustrative example and $\frac{Y_{UF_5}}{Y_{UF_6}}\sim0.927$ (from simple scaling rules), we find for this specific case $\frac{Y}{Y_{UF_6}}\sim0.99988\pm0.00008$, where the 1-σ uncertainty estimated by propagation of

variance assumes a 20% and 5% relative standard deviation in the values of f and $\frac{Y_{UF_5}}{Y_{UF_6}}$, respectively.

Repeating the calculation for 2-, 3-, 4-, and 5-year-old source material by doubling the value of f and so on, we find the following.

Table B-1. Indicative fractional reduction in (α,n) production rate from a HEU sample with age based on the illustrative example discussed in the text.

Age (years)	$\frac{Y}{Y_{UF_6}}$
1	0.99988 ± 0.00008
2	0.99976 ± 0.00016
3	0.99964 ± 0.00024
4	0.99952 ± 0.00032
5	0.99940 ± 0.00040

Recall the choice of HEU was the extreme case and that our main samples are not very old since the last liquid transfer, so we see that the predicted effect of radiolysis is rather modest.

REFERENCES FOR APPENDIX B

[B-1] WD Strunk and SG Thornton (Eds), Uranium Hexafluoride – Safe Handling, Processing, and Transport Conference Proceedings May 24-26, 1988, Oak Ridge, Tennessee, CONF-880558 – DE88 010460 (1988).

[B-2] National Research Council (NRC) Molten Salt Panel of the Committee on Remediation of Buried and Tank Wastes, *Evaluation of the U.S. Department of Energy's Alternatives for the Removal and Disposition of Molten Salt Reactor Experiment Fluoride Salts*, National Academy Press, Washington, DC, 1997. ISBN 0-309-05684-5.

[B-3] JJ Katz and I Sheft, "Halides of the actinide elements," in HJ Emeléus and AG Sharpe (Eds), *Advances in Inorganic Chemistry and Radiochemistry*, Volume 2, Academic Press Inc. (N.Y., 1960) pp195-233.

[B-4] DS Bracken, RS Biddle, LA Carrillo, PA Hypes, CR Rudy, DM Schneider, and MK Smith, *Application Guide to Safeguards Calorimetry*, Los Alamos National Laboratory Manual Report LA-13867-M (January 2002).

[B-5] LD Trowbridge, SH Park, I Remec, and JP Renier, *Technical bases of selection of trapping technology for the MSRE interim vent and trapping project*, Oak Ridge K-25 Site Report K/TCD-1142 (August 1995).

[B-6] AJ Saraceno, "Fluorine overpressurization in the VHE (five-inch) cylinders," Uranium Hexafluoride Conference, CONF-880588(1988) 25-27.

[B-7] NE Bibler, "α and β radiolysis of plutonium hexafluoride vapor," *J. Physical Chemistry* 83(17) (1979) 2179-2186.

[B-8] HA Bernhardt, W Davis Jr., and CH Shiflett, with ME Steidlitz, FD Rosen, and WS Wendolski, "Radiation effects of alpha particles on uranium hexafluoride," Second United Nations International Conference on the Peaceful Uses of Atomic Energy, A/CONF.15/P/522 U.S.A (June 1958) 19 pp.

[B-9] ME Steidlitz, FD Rosen, CH Shiflett, and W Davis, Jr., "Ionization of fluorocarbon gases by uranium-234 α-particles," *J. Physical Chem.* 56 (1952) 1010-1012.

[B-10] VA Dmitrievskii and AI Migachev, "Radiolysis of uranium hexafluoride," UDC 541.15, pp 543-548. Translated from *Atomnaya Énergiya*, No. 5 pp. 438-443, May 1971. Original article submitted February 9, 1970.

[B-11] BNL NNDC Chart of the Nuclides, https://www.nndc.bnl.gov/chart/, accessed 15 April 2018.

See also:

CH Shiflett, ME Steidlitz, FD Rosen, and W Davis, Jr., "The chemical effect of alpha particles on uranium hexafluoride," *J. Inorg. Nucl. Chem.* 7 (1958) 210-233, which is by the same group and covers similar material.

APPENDIX C. STOPPING POWER DATA FOR ALPHA PARTICLES

APPENDIX C. STOPPING POWER DATA FOR ALPHA PARTICLES

Reliable nuclear and atomic data of various kinds are needed for safeguards applications. One type of data often overlooked is the stopping power of alpha particles in materials. The stopping power function governs the slowing down of alpha particles and hence influences both thick-target integrated over angle yield and emission spectrum calculations. Consequently, stopping power data introduces uncertainty into (α,n) source terms and limits how well experimental results for one compound can be scaled to another.

Stopping power theory of ions in matter (not interactions single atoms or molecule) is a rich and difficult basic physics problem that has been the subject of extensive study since the discovery of radioactivity [C-1]. Although stopping powers are heavily relied on for applications [C-2], stopping power theory is by no means completely understood in a single self-consistent unified framework. Early in the 20th century, stopping power theory and experiments helped elucidate the existence and structure of atoms and today requires a deep understanding of the quantum nature of materials. From an applied perspective, stopping power theory also provides a valuable collection of models and a general framework around which to build empirical descriptions to describe experimental stopping power data in a unified way. One way to do this is to build scaling rules from plausible arguments based on the extensive experimental stopping power data of protons and alpha particles evaluated collectively. Using this approach, for the low-energy region (below 10 MeV) of interest to us, Ziegler [C-3] represented the stopping power, S_e, of ^{4}He-ions (α-particles) slowing down in matter as follows.

$$\frac{1}{S_e} = \frac{1}{S_L} + \frac{1}{S_H}\,, \tag{C.1}$$

which, by algebraic rearrangement, is mathematically equivalent to

$$S_e = \frac{S_L \cdot S_H}{S_L + S_H}\,. \tag{C.2}$$

The two *element*-dependent, energy-dependent functions are defined by

$$S_L = A_1 \cdot E^{A_2} \tag{C-3}$$

and

$$S_H = \left(\frac{A_3}{E}\right) \cdot ln\left(1 + \frac{A_4}{E} + A_5 \cdot E\right), \tag{C-4}$$

where E is the kinetic energy of the ^{4}He ion in keV ($E = 1\ to\ 10{,}000\ keV$), $A_1 - A_5$ are fit parameters evaluated against experimental data for elements H to U, and S_e is in units of [eV/(10^{15} atoms/cm^2)]. Below 1 keV, $S_e(E) = S_e(E) \cdot \left(\frac{E}{1}\right)^{A_2} \approx S_L(E)$ may be used, although for our (α,n) problem space this soft energy region is of little practical concern.

The overall stopping power, $S = S_n + S_e$, is represented as the sum of the nuclear and electronic contributions, which, because of the timescales and nature of the interactions, are, to good approximation, distinct physical energy-loss processes. For the *isotope* and energy-dependent nuclear stopping powers, Ziegler [C-3, C-4] used a piecewise continuous universal analytical expression based on the work of Kalbitzer et al. [C-5] formulated in terms of the reduced ion energy, ε, and defined by

$$\varepsilon = \frac{32.53 \cdot M_2 \cdot E}{Z_1 \cdot Z_2 \cdot (M_1 + M_2) \cdot \left({Z_1}^{2/3} + {Z_2}^{2/3}\right)^{1/2}}, \tag{C-5}$$

where $Z_1 = 2$ is the charge of the ^{4}He nucleus and Z_2 is the charge of the target nucleus. Similarly, M_1 and M_2 are the (relative) rest masses of the ^{4}He ion and the target nucleus, conveniently expressed in atomic mass units (u), where 1 u is one-twelfth of the mass of a ^{12}C atom. Because the difference between the atomic and nuclear mass is small, the value of M_2 may reasonably be approximated by the atomic mass. The numerical values used by Ziegler for the universal nuclear stopping power contribution are as follows.

$$\text{For } \varepsilon < 0.01,\ S_n = K \cdot 1.593 \cdot \varepsilon^{1/2}. \tag{C-6}$$

$$\text{For } 0.01 \le \varepsilon \le 10,\ S_n = K \cdot 1.7 \cdot \varepsilon^{1/2} \cdot \frac{ln(e + \varepsilon)}{1 + 6.8 \cdot \varepsilon + 3.4 \cdot \varepsilon^{3/2}},\ \text{where } e = \exp(1). \tag{C-7}$$

For $\varepsilon > 10$, $S_n = K \cdot \frac{ln(0.47 \cdot \varepsilon)}{2 \cdot \varepsilon}$, and while Zeigler gives no upper limit, Kalbitzer et al. say $\varepsilon \le 100$.

The target-specific conversion constant K is given by

$$K = \frac{8.462 \cdot Z_1 \cdot Z_2 \cdot M_1}{(M_1 + M_2) \cdot \left({Z_1}^{2/3} + {Z_2}^{2/3}\right)^{1/2}}, \tag{C-8}$$

and the units of S_n are [eV/(10^{15} atoms/cm^2)]. The different authors agree that the accuracy of the representation is difficult to assess. Experimental evidence is often scarce and in disagreement. We are

reluctant to offer advice from the general to the specific but guess a systematic uncertainty of the order of 20% for the nuclear stopping contribution.

Stopping powers based on the treatment of Ziegler [C-3, C-4] are incorporated into the SOURCES4C computer code. However, Ziegler and his colleagues have updated the stopping power treatment, and it is now maintained in the SRIM code [C-6]. It is our view that this advance needs to be fully incorporated into SOURCES4C and the impact of the change evaluated. Note that the universal nuclear stopping power treatment in SRIM-2013 was changed to

$$\varepsilon = \frac{32.53 \cdot M_2 \cdot E}{Z_1 \cdot Z_2 \cdot (M_1 + M_2) \cdot \left({Z_1}^{0.23} + {Z_2}^{0.23}\right)} \cdot \tag{C-9}$$

$$\text{For } \varepsilon \leq 30,\ S_n = K \cdot \frac{\frac{1}{2} \cdot ln(1 + 1.1383\varepsilon)}{1 + 0.01321 \cdot \varepsilon^{0.21226} + 0.19593 \cdot \varepsilon^{0.5}} \cdot \tag{C-10}$$

$$\text{For } \varepsilon > 30,\ S_n = K \cdot \frac{\frac{1}{2} \cdot ln(\varepsilon)}{\varepsilon} \cdot \tag{C-11}$$

$$K = \frac{8.462 \cdot Z_1 \cdot Z_2 \cdot M_1}{(M_1 + M_2) \cdot \left({Z_1}^{0.23} + {Z_2}^{0.23}\right)} \cdot \tag{C-12}$$

Stopping powers for solid-F, Pb, Th, and U are calculated in the Excel spreadsheet Croft - Ziegler 1977.xlsx using Ziegler's parameter set and are compared with the tabulated values. For illustration the numerical values of $A_1 - A_5$ for solid-^{19}F are taken to be 1.533, 0.531, 40440, 18410, and 0.002718, respectively. $Z_1 = 2$, $M_1 = 4.001506179127$, $Z_2 = 9$, and $M_2 = 18.998403$. Note that for Pb, Th, and U, the nuclear stopping was approximated using a single calculation with the average atomic mass.

Stopping powers can be readily calculated using the SRIM utility on an arbitrary energy grid for interpolation, and this may be an alternative way for SOURCES4C to store and use the up-to-date stopping power data. In a favorable case, accuracies for the kinds of applications we are considering here can be expected to be in the 1–3% range.

SOURCE4C must have the architecture and capability to deal with the full range of (α,n) targets and materials (e.g., for safeguards applications Z = 3–19 up to 10 MeV is a minimal requirement), but for the present problem a considerable simplification is possible because the energy range of interest extends from the F(α,n) reaction threshold at about 2.364 MeV [which can be estimated using the Qtool utility at https://t2.lanl.gov/nis/data/qtool.html] where bonding and phase effects are less consequential and (being

above the peak) the energy dependence is falling gradually and monotonically. The alpha spectrum from naturally occurring uranium nuclides is also quite soft, extending to only 4.775 MeV [this is the upper value for ^{234}U; see BNL NNDC Chart of the Nuclides (https://www.nndc.bnl.gov/chart/)].

Phase and bonding effects are notoriously difficult to account for in a general way [C-7]. In using SRIM for UF_6, we adopt the stopping power of fluorine in the solid phase because below about 5 MeV the difference is expected to be significant.

We assume Bragg-Kleeman (B-K) additivity (that is that atomic contributions are independent). There are no firm rules for estimating what the effect of chemical bonding might have, although for compounds involving heavy metals we anticipate B-K to underestimate the stopping power by less that about 2% at 500 keV. Above about 2 MeV the effect should be quite small (recall the F(α,n) threshold is at 2.356 MeV).

Interpreting thin target data stopping power introduces an additional uncertainty because the way the target is made may make a difference (based on notionally high-accuracy stopping power data collected on foil, sputtered, and evaporated materials [SRIM]) with different microscopic amorphous and crystalline structures.

For thick-target yield calculations for an internal α-emitter, backscattering is not important as α's are neither lost nor gained but merely redirected. In thin target measurements, backscatter from the front leads to loss and a partial yield contribution that may not contribute to collected charge but is small as the target deposit itself is small; backscatter of the backing may about double the yield contribution and again not be collected electrically.

Above Z = 92 there is no reliable systematic data, and SRIM does not extrapolate beyond uranium. If we assume that the dominant influence is on the stopping power cross section is reflected in the Z-dependence, then one thing to try is to scale the stopping power cross section for transuranic metals from that for uranium as follows.

$$X(Z = 92 + n) \approx \left[\frac{X(92)}{X(92 - n)}\right] \cdot X(92)\ , \qquad \text{(C-13)}$$

so, for example,

$$X(Pu) \approx \left[\frac{X(U)}{X(Th)}\right] \cdot X(U)\ .$$

REFERENCES FOR APPENDIX C

[C-1] H Bichsel, DE Groom, and SR Klein, "Passage of particles through matter, section 33 under Experimental Methods and Colliders," in Particle Data Group: Reviews, Tables, Plots, M Tanabashi et al. (Particle Data Group), *Review of Particle Physics Phys. Rev*. D98, 030001 (2018), available online at http://pdg.lbl.gov/2018/reviews/contents_sports.html

[C-2] W-K Chu, JW Mayer, and M-A Nicolet, *Backscattering Spectrometry*, Academic Press (1978). ISBN 0-12-173850-7.

[C-3] JF Ziegler, *Helium Stopping Powers and Ranges in All Elemental matter*, Volume 4 of *The Stopping and Ranges of Ions in Matter*, organized by J.F. Ziegler, Pergamon Press Inc. (1977). ISBN 0-08-021606-4.

Stopping powers are usually better thought of as being functions of ion speed rather than energy although keV/amu, is often used in graphs and tables to provide speed dependent behavior. For practical applications when we are concerned with only a single ion type, in this case α-particles, it is convenient to work in terms of kinetic energy. In our energy domain keV/amu is proportional to the ion speed squared.

[C-4] JF Ziegler, "The Electronic and Nuclear Stopping of Energetic Ions," *Applied Physics Letters* 31(1977b) 544-546.

[C-5] S Kalbitzer, H Oetzmann, H Grahmann, and A Feuerstein, "A Simple Universal Fit Formula to Experimental Nuclear Stopping Power Data," *Zeitschrift für Physik* A278 (1976) 223-224.

Note that the parameters given by Kalbitzer for the nuclear stopping power result in a discontinuous representation, so Zeigler used different parameters. It is interesting to see the size of the changes. In the original work Kalbitzer et al. had for the three energy regions

$$S_n = K \cdot 1.7 \cdot \varepsilon^{1/2},$$

$$S_n = K \cdot a_1 \cdot \varepsilon^{1/2} \cdot \frac{ln(e + \varepsilon)}{1 + a_2 \cdot \varepsilon + a_3 \cdot \varepsilon^{3/2}}, \text{ and}$$

$$\frac{ln(1 \cdot \varepsilon)}{2 \cdot \varepsilon},$$

where $a_1 = 1.7$, $a_2 \approx 4 \cdot a_1$ *and chosen to be* $\sim 6.4 \pm 1.7$ *to cover the experimental data, and* $a_3 = 2 \cdot a_1 = 3.4$. *Numerically the parameters for the central energy zone are the same as those used by Zeigler but, there are differences for the other two zones*.

SOURCES4C

[C-6] JF Ziegler, JP Biersack, and MD Ziegler, *SRIM The Stopping and Range of Ions in Matter*, Edition 7, SRIM Co., (2008). ISBN: 0-9654207-1-X. See also www.SRIM.org.

[C-7] JF Ziegler and JM Manoyan, "The Stopping of Ions in Compounds, Nuclear Instruments and Methods," *Physics Research* B35 (1988) 215-228.

H Tai, H Bichsel, JW Wilson, JL Shinn, FA Cucinotta, and FF Badavi, *Comparison of stopping power and range databases for radiation transport study*, U.S. National Aeronautics and Space Administration report, NASA Technical Paper 3644 (October 1997).

See also: SRIM.org/SRIM/compounds

For H, C, N, O, F, S and Cl, some approximate rules, especially for organic compounds and gases, have been constructed, but no guidance exits for Li, Be, and B, which are other strong (α,n) emitters. For example, BN has been used as a target.